UNIVERSITÀ POLITECNICA DELLE MARCHE
Repository ISTITUZIONALE

A Structural Matrix Autoregressive Model for the Joint Dynamics of Volume, Volatility, and Returns

This is a pre print version of the following article:

Original
A Structural Matrix Autoregressive Model for the Joint Dynamics of Volume, Volatility, and Returns / Bucci, A., Palomba, G., Rossi, E.. - ELETTRONICO. - 2606.08141:(2026), pp. 1-37. [Epub ahead of print] [10.48550/arXiv.2606.08141]

Availability:
This version is available at: 11566/359452 since: 2026-06-23T16:27:21Z

Publisher:
Cornell University

Published
DOI:10.48550/arXiv.2606.08141

Terms of use:

The terms and conditions for the reuse of this version of the manuscript are specified in the publishing policy. The use of copyrighted works requires the consent of the rights' holder (author or publisher). Works made available under a Creative Commons license or a Publisher's custom-made license can be used according to the terms and conditions contained therein. See editor's website for further information and terms and conditions.
This item was downloaded from IRIS Università Politecnica delle Marche (https://iris.univpm.it). When citing, please refer to the published version.

(Article begins on next page)

14 September 2026

arXiv:2606.08141v1 [econ.EM] 6 Jun 2026

A Structural Matrix Autoregressive Model for the Joint Dynamics of Volume, Volatility, and Returns

Andrea Bucci[1], Giulio Palomba[2], and Eduardo Rossi[3]

[1]Department of Economics and Law, University of Macerata, Italy
[2]Department of Economics and Social Sciences, Marche Polytechnic University, Italy
[3]Department of Economics and Management, University of Pavia, Italy

Abstract

This paper proposes a Structural Matrix Autoregressive (SMAR) model for the joint analysis of asset returns, realized volatility, and trading volume in a large-dimensional setting. This framework simultaneously captures dynamic spillovers across financial variables and cross-sectional dependence across assets while preserving a parsimonious parameterization relative to conventional vector autoregressive models. The model is estimated on daily data for the constituents of the Dow Jones Industrial Average over the period 2021–2025 and is structurally identified through restrictions consistent with the Mixture of Distributions Hypothesis and efficient market theory. The empirical findings indicate that volatility is the primary driver of trading activity, suggesting that informational shocks are predominantly incorporated into markets through price variability. Forecast error variance decompositions further reveal that, although internal shocks dominate short-term volume dynamics, cross-asset spillovers account for more than 50% of trading volume variation at longer horizons. Finally, an event-study analysis around FOMC announcements supports the proposed decomposition by identifying significant increases in the informative component of trading activity on announcement days followed by rapid mean reversion.

Keywords: Matrix-valued time series; Volatility; Trading volume decomposition; Structural model; MDH

1 Introduction

Recent global history has shown how extreme events cause financial markets to jitter, which experience periods of high volatility and extremely variable trading volumes (see Longin and Solnik, 2001; Diebold and Yilmaz, 2009; Bollerslev et al., 2018). In this context, it is crucial for market participants, institutions, and policymakers to understand how volatility and liquidity spillovers interact (Acharya and Pedersen, 2005; Brunnermeier and Pedersen, 2009). Indeed, while from a microeconomic perspective, understanding the dynamics and correlations of asset prices leads investors and asset managers to portfolio optimization, asset management, and risk hedging, from a macroeconomic perspective, it should lead policymakers towards strategies aimed at economic and financial stability.

Although traditional financial theories have primarily focused on the dynamics between asset prices and their volatility, the analysis of trading volumes has received relatively less attention, despite being an indicator of market sentiment (Darolles et al., 2015). For example, price increases during periods of low volume may only produce transitory effects, while similar price movements during periods of high volume may have long-lasting implications. As further discussed in Bollerslev et al. (2018), trading volume and return volatility tend to co-vary (Chiang et al., 2010), especially after news shocks. This result underlies the common practice of using trading volume as an exogenous regressor in time varying volatility models.

Furthermore, the mixed distribution hypothesis (MDH), initially formulated by Tauchen and Pitts (1983), posits that the observed joint behavior between asset volatility and trading volumes is due to latent information flows that simultaneously drive price fluctuations and trading activity. In parallel, Darolles et al. (2015) emphasize the methodological challenges in jointly modeling price dynamics and trading volumes, particularly when one wants to separate the dynamics related to information shocks from those attributable to liquidity

constraints. These insights point to the necessity of extending existing approaches to better capture the complex dynamics underlying trading activity. In this direction, He and Velu (2014) develop a multi-asset mixture distribution hypothesis model to investigate commonality in stock returns and trading volumes based on factor structure for returns and trading volumes.

Although existing methodologies reliably assess the liquidity-volatility relationship for individual stocks (Chordia et al., 2000; Pástor and Stambaugh, 2003), they overlook different components of liquidity dynamics. To fill this gap in the literature, we propose here to model the cross-asset dynamics of volatility, volumes and prices through the Structural Matrix-valued AutoRegressive (SMAR) model. This method extends the structural vector autoregressive (SVAR) model of Sims (1980) to multivariate settings in which data form matrices. As in the MAR model introduced by Chen et al. (2021), we collect m assets in the rows and n financial metrics in the columns, thus forming a data matrix for each time $t = 1, 2, \ldots, T$. In this way, SMAR jointly takes into account the spillover effects across assets and the dynamic interconnectedness of some financial variables that share a common latent structure in the MDH. The SMAR offers a parsimonious alternative to the traditional architectures, typically the Structural VAR (SVAR) or Panel VAR (PVAR, see Canova and Ciccarelli, 2013, for a comprehensive survey) models, in which matrix data are stacked into a vector. In fact, excluding any deterministic component, the vectorization in these models foresees the estimation of m^2n^2 parameters per lag, while the number of parameters in the SMAR reduces to $m^2 + n^2$. Hence, the vectorization results in a loss of efficiency since the relationships between rows and columns can no longer be maintained, and makes the estimation computationally cumbersome. In addition, while identifying structural innovations in panel SVAR models typically requires computationally intensive data-pooling or the assumption of statistical independence on a massive $mn \times mn$ covariance matrix $\mathbf{\Sigma}$ (e.g., Herwartz and Wang, 2024), the SMAR framework leverages a separable covariance

structure $\mathbf{\Sigma} = \mathbf{\Sigma}_{\mathrm{r}} \otimes \mathbf{\Sigma}_{\mathrm{c}}$, where $\mathbf{\Sigma}_{\mathrm{c}}$ and $\mathbf{\Sigma}_{\mathrm{r}}$ are the column- and row-wise error covariance matrices. This allows one to perform simultaneous structural identification exclusively within the lower-dimensional $n \times n$ variable space $\mathbf{\Sigma}_{\mathrm{c}}$, leaving cross-sectional dependencies to be absorbed by $\mathbf{\Sigma}_{\mathrm{r}}$ without requiring restrictive entity-level orderings. Furthermore, we can exploit the algebraic properties of our framework to solve analytically the identification issues and compute both single-asset-single-variable impulse response functions (IRFs) and averaged IRFs across either assets or financial variables. In addition, since our approach relies on the explicit structural impulse response functions, they represent a valid alternative to those defined by Chen et al. (2021) in the MAR context.

We apply the SMAR model to daily data for $m = 30$ assets composing the Dow Jones index, covering the period from January 2021 to February 2025. The empirical analysis delivers several findings. First, volatility is a key determinant of trading activity. Second, a forecast error variance decomposition suggests that trading volume is primarily driven by its own shocks over the short run, while cross-asset spillovers account for more than half of the total volume variance over a 20-day time horizon. Moreover, an event study around the announcements of the Federal Open Market Committee (FOMC) shows a statistically significant spike in the information share of volume on announcement days (Lucca and Moench, 2015), followed by a rapid mean reversion consistent with efficient price discovery (Andersen et al., 2003).

The remainder of the paper is organized as follows. In Section 2, we introduce the SMAR model, discuss identification issues, and define the impulse response functions. Section 3 proposes a specification of the column-wise structural matrix based on some results from the finance literature and provides some financial considerations. Section 4 is devoted to the empirical analysis, and finally Section 5 concludes.

2 The Structural MAR model

Let $\mathbf{Y}_t$ be a time series matrix $m \times n$, with $t = 1, 2, \ldots, T$, containing data for m assets and n financial measures. Since we are interested in a structural model that incorporates simultaneous relationships between all row and column variables of $\mathbf{Y}_t$, these simultaneous interactions are represented in a linear setup by the $m \times m$ matrix $\mathbf{R}_0$ and the $(n \times n)$ matrix $\mathbf{C}_0$, both of full rank. Therefore, the structural MAR(p) model (hereafter SMAR) is defined as

$$\mathbf{R}_0 \mathbf{Y}_t \mathbf{C}_0^\top = \mathbf{R}_1 \mathbf{Y}_{t-1} \mathbf{C}_1^\top + \cdots + \mathbf{R}_p \mathbf{Y}_{t-p} \mathbf{C}_p^\top + \mathbf{U}_t, \tag{1}$$

where p is the lag order, $\mathbf{R}_1, \ldots, \mathbf{R}_p$ are $m \times m$ row-wise effect parameter matrices whose Frobenius norm must be equal to 1 (see Chen et al., 2021), $\mathbf{C}_1, \ldots, \mathbf{C}_p$ are $n \times n$ matrices containing the parameters for column-wise relationships. The deterministic components have been suppressed for notational convenience. $\mathbf{U}_t$ denotes an $m \times n$ matrix of serially uncorrelated structural shocks with zero mean and unit variances (Kilian and Lüktepohl, 2017). It follows that the $mn \times mn$ covariance matrix of vec($\mathbf{U}_t$) (where the vec operator transforms a matrix into a vector by stacking the columns of the matrix one underneath the other) is the identity matrix

$$\mathbf{\Omega} = \mathrm{Var}\left(\mathrm{vec}(\mathbf{U}_t)\right) = \mathbf{I}_{mn} = \mathbf{I}_n \otimes \mathbf{I}_m, \tag{2}$$

where $\mathbf{I}_m$ and $\mathbf{I}_n$ represent the row-wise and the column-wise covariance matrices, respectively. Therefore, there are as many structural shocks as variables in the model, and these shocks are mutually uncorrelated with unit variance (Kilian and Lüktepohl, 2017).

The reduced-form representation of the structural MAR(p) model, *i.e.*, where $\mathbf{Y}_t$ is a function of the lags of $\mathbf{Y}_t$ only, is obtained by post-multiplying both sides of Equation (1) by $\mathbf{C}_0^{-\top}$ and pre-multiplying by $\mathbf{R}_0^{-1}$. This leads to

$$\mathbf{R}_0^{-1}\mathbf{R}_0 \mathbf{Y}_t \mathbf{C}_0^\top \mathbf{C}_0^{-\top} = \mathbf{R}_0^{-1}\mathbf{R}_1 \mathbf{Y}_{t-1} \mathbf{C}_1^\top \mathbf{C}_0^{-\top} + \cdots + \mathbf{R}_0^{-1}\mathbf{R}_p \mathbf{Y}_{t-p} \mathbf{C}_p^\top \mathbf{C}_0^{-\top} + \mathbf{R}_0^{-1}\mathbf{U}_t \mathbf{C}_0^{-\top},$$

that corresponds to the reduced-form MAR(p) by Chen et al. (2021) given by

$$\mathbf{Y}_t = \mathbf{A}_1\mathbf{Y}_{t-1}\mathbf{B}_1^\top + \cdots + \mathbf{A}_p\mathbf{Y}_{t-p}\mathbf{B}_p^\top + \mathbf{E}_t, \tag{3}$$

where $\mathbf{A}_i = \mathbf{R}_0^{-1}\mathbf{R}_i$ are $m \times m$ matrices, and $\mathbf{B}_i = \mathbf{C}_0^{-1}\mathbf{C}_i$ are $n \times n$ matrices for $\forall\, i = 1, \ldots, p$. Consequently, the reduced-form innovation matrix at time t is given by

$$\mathbf{E}_t = \mathbf{R}_0^{-1}\mathbf{U}_t\mathbf{C}_0^{-\top}. \tag{4}$$

To compute the covariance of $\mathbf{E}_t$, we can use the vectorized form of Equation (1), given by

$$(\mathbf{C}_0 \otimes \mathbf{R}_0)\text{vec}(\mathbf{Y}_t) = (\mathbf{C}_1 \otimes \mathbf{R}_1)\text{vec}(\mathbf{Y}_{t-1}) + \cdots + (\mathbf{C}_p \otimes \mathbf{R}_p)\text{vec}(\mathbf{Y}_{t-p}) + \text{vec}(\mathbf{U}_t). \tag{5}$$

Since $\mathbf{R}_0$ and $\mathbf{C}_0$ are nonsingular, pre-multiplying by $(\mathbf{C}_0 \otimes \mathbf{R}_0)^{-1}$ implies that

$$\begin{aligned}\text{vec}(\mathbf{Y}_t) = (\mathbf{C}_0 \otimes \mathbf{R}_0)^{-1}(\mathbf{C}_1 \otimes \mathbf{R}_1)\text{vec}(\mathbf{Y}_{t-1}) + \\ + \cdots + (\mathbf{C}_0 \otimes \mathbf{R}_0)^{-1}(\mathbf{C}_p \otimes \mathbf{R}_p)\text{vec}(\mathbf{Y}_{t-p}) + (\mathbf{C}_0 \otimes \mathbf{R}_0)^{-1}\text{vec}(\mathbf{U}_t).\end{aligned} \tag{6}$$

Further, we can obtain

$$\text{vec}(\mathbf{E}_t) = \text{vec}\left(\mathbf{R}_0^{-1}\mathbf{U}_t\mathbf{C}_0^{-\top}\right) = \left[\mathbf{C}_0^{-1} \otimes \mathbf{R}_0^{-1}\right]\text{vec}(\mathbf{U}_t).$$

Considering the covariance matrix of structural shocks defined by the equation (2), the covariance matrix of vec($\mathbf{E}_t$) turns out to be

$$\boldsymbol{\Sigma}_E = \left[\mathbf{C}_0^{-1} \otimes \mathbf{R}_0^{-1}\right]\boldsymbol{\Omega}\left[\mathbf{C}_0^{-1} \otimes \mathbf{R}_0^{-1}\right]^\top = \left(\mathbf{C}_0^\top\mathbf{C}_0\right)^{-1} \otimes \left(\mathbf{R}_0^\top\mathbf{R}_0\right)^{-1}. \tag{7}$$

Assuming that the covariance of $\mathbf{E}_t$ in a MAR model (Chen et al., 2021) is an $mn \times mn$ matrix expressed as

$$\boldsymbol{\Sigma}_E = \boldsymbol{\Sigma}_\text{c} \otimes \boldsymbol{\Sigma}_\text{r},$$

it follows that the term $\boldsymbol{\Sigma}_\text{c} = \left(\mathbf{C}_0^\top\mathbf{C}_0\right)^{-1}$ represents the column-wise covariance of $\mathbf{E}_t$, while $\boldsymbol{\Sigma}_\text{r} = \left(\mathbf{R}_0^\top\mathbf{R}_0\right)^{-1}$ denotes the row-wise covariance of $\mathbf{E}_t$. In this context, the column-wise and row-wise covariance matrices of the reduced-form error, $\boldsymbol{\Sigma}_\text{c}$ and $\boldsymbol{\Sigma}_\text{r}$, can be considered known (Kilian and Lüktepohl, 2017).

2.1 Identification

For the identification of $\mathbf{C}_0^{-\top}$, it can be noticed that the number of free parameters in $\mathbf{\Sigma}_\mathrm{c}$ is $n(n+1)/2$ which is the upper limit for the number of parameters in $\mathbf{C}_0^{-\top}$ that can be uniquely identified (Kilian and Lüktepohl, 2017). This means that we have to impose at least $n(n-1)/2$ normalizing restrictions.

Since $\mathbf{\Sigma}_\mathrm{c}^{-1} = \mathbf{C}_0^\top \mathbf{C}_0$, we can assume that $\mathbf{C}_0^\top$ is a lower triangular matrix with positive diagonal elements, as in the following section, *i.e.*, the Cholesky factor of $\mathbf{\Sigma}_\mathrm{c}^{-1}$.

Analogously, given that $\mathbf{\Sigma}_\mathrm{r}$ has $m(m+1)/2$ unique elements, we must impose $m(m-1)/2$ conditions to achieve identification of the parameters of $\mathbf{R}_0$. This means that, in our model, identifying contemporaneous effects across assets can be challenging, as the number of required constraints increases quadratically with the number of assets (m). Defining such a large number of constraints from economic theory is often very difficult, as the simultaneous interactions between different assets could be extremely complex.

While we recognize that constraints can be imposed in the Equation (1) by dividing assets into clusters using appropriate techniques (*e.g.*, cluster analysis or principal components analysis), or by adopting some criterion to separate the elements (*e.g.*, sector or return on assets), we assume that contemporaneous changes are due exclusively to structural shocks to financial measures, rather than being specific to individual assets; in practice, we impose the structure $\mathbf{R}_0 = \mathbf{I}_m$.

2.2 SMAR model estimation

In this section, we present the log-likelihood of the SMAR(1) model. We start by defining the set of parameters contained in the vector $\boldsymbol{\psi} = \left[\mathrm{vec}(\mathbf{C}_0)^\top, \mathrm{vec}(\mathbf{C}_1)^\top, \mathrm{vec}(\mathbf{R}_0)^\top, \mathrm{vec}(\mathbf{R}_1)^\top\right]^\top$. The Gaussian log-likelihood (Wu and Chan, 2026) is

$$\ell(\boldsymbol{\psi}; \mathbf{Y}_t, \mathbf{Y}_{t-1}) = -\frac{m}{2}(T-1)\log|\mathbf{\Sigma}_\mathrm{c}| - \frac{n}{2}(T-1)\log|\mathbf{\Sigma}_\mathrm{r}| - \frac{1}{2}\sum_{t=2}^{T}\mathrm{tr}\left(\mathbf{\Sigma}_\mathrm{r}^{-1}\mathbf{E}_t\mathbf{\Sigma}_\mathrm{c}^{-1}\mathbf{E}_t^\top\right), \quad (8)$$

where

$$\mathbf{E}_t = \mathbf{Y}_t - (\mathbf{R}_0^{-1}\mathbf{R}_1)\mathbf{Y}_{t-1}(\mathbf{C}_0^{-1}\mathbf{C}_1)^\top. \tag{9}$$

Given that $\mathbf{U}_t = \mathbf{R}_0\mathbf{Y}_t\mathbf{C}_0^\top - \mathbf{R}_1\mathbf{Y}_{t-1}\mathbf{C}_1^\top$, the first-order derivatives with respect to $\mathbf{R}_0, \mathbf{R}_1, \mathbf{C}_0$ and $\mathbf{C}_1$ are given by

$$\begin{aligned}
\frac{\partial \ell(\cdot)}{\partial \mathbf{R}_0} &= n(T-1)\mathbf{R}_0^{-\top} - \sum_{t=2}^{T} \mathbf{U}_t\mathbf{C}_0\mathbf{Y}_t^\top \\
\frac{\partial \ell(\cdot)}{\partial \mathbf{R}_1} &= \sum_{t=2}^{T} \mathbf{U}_t\mathbf{C}_1\mathbf{Y}_{t-1}^\top \\
\frac{\partial \ell(\cdot)}{\partial \mathbf{C}_0} &= m(T-1)\mathbf{C}_0^{-\top} - \sum_{t=2}^{T} \mathbf{Y}_t^\top\mathbf{R}_0^\top\mathbf{U}_t \\
\frac{\partial \ell(\cdot)}{\partial \mathbf{C}_1} &= \sum_{t=2}^{T} \mathbf{Y}_{t-1}^\top\mathbf{R}_1^\top\mathbf{U}_t.
\end{aligned} \tag{10}$$

Since the first-order conditions for $\mathbf{C}_0$ and $\mathbf{R}_0$ do not have an analytic solution, the parameters can be estimated by numerical optimization. However, this is hampered by the dimension of $\mathbf{C}_0$ and $\mathbf{R}_0$ which makes this approach unfeasible, especially for high-dimensional problems. Alternatively, one can rely on the iterative estimation (Chen et al., 2021) of $\mathbf{A}_1, \mathbf{B}_1, \mathbf{\Sigma}_\text{c}, \mathbf{\Sigma}_\text{r}$, often referred to as the "flip-flop" algorithm (see Dutilleul, 1999). In this case, only one matrix is updated, while keeping fixed the others using the following iterations

$$\begin{aligned}
\mathbf{A}_1 &\leftarrow \left(\sum_{t=2}^{T} \mathbf{Y}_t\mathbf{\Sigma}_\text{c}^{-1}\mathbf{B}_1\mathbf{Y}_{t-1}^\top\right)\left(\sum_{t=2}^{T} \mathbf{Y}_{t-1}\mathbf{B}_1^\top\mathbf{\Sigma}_\text{c}^{-1}\mathbf{B}_1\mathbf{Y}_{t-1}^\top\right)^{-1} \\
\mathbf{B}_1 &\leftarrow \left(\sum_{t=2}^{T} \mathbf{Y}_t^\top\mathbf{\Sigma}_\text{r}^{-1}\mathbf{A}_1\mathbf{Y}_{t-1}\right)\left(\sum_{t=2}^{T} \mathbf{Y}_{t-1}^\top\mathbf{A}_1^\top\mathbf{\Sigma}_\text{r}^{-1}\mathbf{A}_1\mathbf{Y}_{t-1}\right)^{-1} \\
\mathbf{\Sigma}_\text{c} &\leftarrow \frac{\sum_{t=2}^{T} \mathbf{E}_t^\top\mathbf{\Sigma}_\text{r}^{-1}\mathbf{E}_t}{m(T-1)} \\
\mathbf{\Sigma}_\text{r} &\leftarrow \frac{\sum_{t=2}^{T} \mathbf{E}_t\mathbf{\Sigma}_\text{c}^{-1}\mathbf{E}_t^\top}{n(T-1)},
\end{aligned} \tag{11}$$

where $\mathbf{A}_1$ and $\mathbf{\Sigma}_\text{r}$ have a unit Frobenius norm (see Chen et al., 2021; Bucci et al., 2026, for details). Since we impose $\mathbf{R}_0 = \mathbf{I}_m$ in Section 2.1, here we focus only on $\mathbf{C}_0$. We can

recover $\hat{\mathbf{C}}_0^\top$ as the Cholesky factor of the estimated inverse of $\boldsymbol{\Sigma}_{\mathrm{c}}$, *i.e.*,

$$\hat{\boldsymbol{\Sigma}}_{\mathrm{c}}^{-1} = \hat{\mathbf{C}}_0^\top \hat{\mathbf{C}}_0. \tag{12}$$

For the purpose of interpretability, we normalize the effect of the structural shocks on the errors of the reduced-form model as follows:

$$\hat{\mathbf{Q}} = \hat{\mathbf{C}}_0 \langle \hat{\mathbf{C}}_0 \rangle^{-1} \tag{13}$$

where $\langle \hat{\mathbf{C}}_0 \rangle = \mathrm{diag}(\hat{\mathbf{C}}_0)$.

Using the following total score for $\boldsymbol{\beta} = \left[\mathrm{vec}(\mathbf{A}_1)^\top, \mathrm{vec}(\mathbf{B}_1)^\top, \mathrm{vech}(\boldsymbol{\Sigma}_{\mathrm{r}})^\top, \mathrm{vech}(\boldsymbol{\Sigma}_{\mathrm{c}})^\top\right]^\top$, $s_T(\boldsymbol{\beta}) = \sum_{t=2}^T s_t(\boldsymbol{\beta})$ (where vech is the operator that stacks the lower triangular elements of a matrix in a vector), derived in Appendix A

$$\mathbf{s}_T(\boldsymbol{\beta}) = \begin{bmatrix} \frac{\partial \ell(\cdot)}{\partial \mathrm{vec}(\mathbf{A}_1)} \\ \frac{\partial \ell(\cdot)}{\partial \mathrm{vec}(\mathbf{B}_1)} \\ \frac{\partial \ell(\cdot)}{\partial \mathrm{vech}(\boldsymbol{\Sigma}_{\mathrm{c}})} \\ \frac{\partial \ell(\cdot)}{\partial \mathrm{vech}(\boldsymbol{\Sigma}_{\mathrm{r}})} \end{bmatrix} = \begin{bmatrix} \sum_{t=2}^T \left[(\mathbf{Y}_{t-1}\mathbf{B}_1^\top \boldsymbol{\Sigma}_{\mathrm{c}}^{-1}) \otimes \boldsymbol{\Sigma}_{\mathrm{r}}^{-1}\right] \mathrm{vec}(\mathbf{E}_t) \\ \sum_{t=2}^T \left[(\mathbf{Y}_{t-1}^\top \mathbf{A}_1^\top \boldsymbol{\Sigma}_{\mathrm{r}}^{-1}) \otimes \boldsymbol{\Sigma}_{\mathrm{c}}^{-1}\right] \mathrm{vec}(\mathbf{E}_t^\top) \\ -\frac{m}{2}(T-1)\mathbf{D}_n^\top \mathrm{vec}(\boldsymbol{\Sigma}_{\mathrm{c}}^{-1}) + \frac{1}{2}\sum_{t=2}^T \mathbf{D}_n^\top (\boldsymbol{\Sigma}_{\mathrm{c}}^{-1} \otimes \boldsymbol{\Sigma}_{\mathrm{c}}^{-1}) \mathrm{vec}(\mathbf{E}_t^\top \boldsymbol{\Sigma}_{\mathrm{r}}^{-1} \mathbf{E}_t) \\ -\frac{n}{2}(T-1)\mathbf{D}_m^\top \mathrm{vec}(\boldsymbol{\Sigma}_{\mathrm{r}}^{-1}) + \frac{1}{2}\sum_{t=2}^T \mathbf{D}_m^\top (\boldsymbol{\Sigma}_{\mathrm{r}}^{-1} \otimes \boldsymbol{\Sigma}_{\mathrm{r}}^{-1}) \mathrm{vec}\left(\mathbf{E}_t \boldsymbol{\Sigma}_{\mathrm{c}}^{-1} \mathbf{E}_t^\top\right) \end{bmatrix}, \tag{14}$$

where $\mathbf{D}_n$ is the duplication matrix that projects from the n-dimensional space onto the $n(n+1)/2$-dimensional space (the same is for $\mathbf{D}_m$), *i.e.*, $\mathrm{vec}(\mathbf{X}) = \mathbf{D}_n \mathrm{vech}(\mathbf{X})$. We can compute the asymptotic covariance matrix for the reduced-form parameters with the Fisher's Information matrix

$$\boldsymbol{\mathcal{I}}(\boldsymbol{\beta}) = \mathbb{E}\left[\mathbf{s}_t(\boldsymbol{\beta})\mathbf{s}_t(\boldsymbol{\beta})^\top\right]$$

which, under regularity conditions, asymptotically converges to $-\mathbb{E}[\boldsymbol{\mathcal{H}}(\boldsymbol{\beta})]$, where $\boldsymbol{\mathcal{H}}(\boldsymbol{\beta})$ is the Hessian matrix of the log-likelihood function. Therefore, evaluating the score at the optimum, we can estimate the asymptotic covariance matrix using the outer-product-of-gradients (OPG) estimator $\widehat{\mathrm{Var}}(\hat{\boldsymbol{\beta}}) = \left[\sum_{t=2}^T \mathbf{s}_t(\hat{\boldsymbol{\beta}})\mathbf{s}_t(\hat{\boldsymbol{\beta}})^\top\right]^{-1}$.

In our case, we need to find the standard errors of the structural impact parameters. Since the structural matrix $\mathbf{Q}^{-\top}$ is a non-linear transformation of the reduced-form pa-

rameters, the standard errors of $\hat{\mathbf{Q}}^{-\top}$ are computed via the delta method[1]. To this end, we define the $n(n-1)/2$-dimensional vector containing the sub-diagonal elements of $\hat{\mathbf{Q}}^{-\top}$, $\text{vecl}(\hat{\mathbf{Q}}^{-\top})$. Proposition 1 provides the Jacobian of $\text{vecl}(\hat{\mathbf{Q}}^{-\top})$ with respect to $\text{vech}(\hat{\mathbf{\Sigma}}_c)$.

Proposition 1. *Let $\hat{\mathbf{\Sigma}}_c$ be the ML estimate of the reduced-form column covariance matrix, $\hat{\mathbf{C}}_0 = \text{chol}(\hat{\mathbf{\Sigma}}_c^{-1})$ its upper triangular Cholesky factor, and $\hat{\mathbf{Q}} = \hat{\mathbf{C}}_0\langle\hat{\mathbf{C}}_0\rangle^{-1}$ the structural unit upper triangular matrix, where $\langle\hat{\mathbf{C}}_0\rangle = \text{diag}(\hat{\mathbf{C}}_0)$. The Jacobian $\mathbf{J} = \frac{\partial\ \text{vecl}(\hat{\mathbf{Q}}^{-\top})}{\partial\ \text{vech}(\hat{\mathbf{\Sigma}}_c)^\top}$ is*

$$\mathbf{J} = \mathbf{L}_n^s \left[\left(\hat{\mathbf{Q}}^{-1} \otimes \hat{\mathbf{C}}_0^{-\top}\right) - \sum_{k=1}^{n} \left(\mathbf{H}_k \otimes \hat{\mathbf{C}}_0^{-\top}\mathbf{H}_k\right) \right] \mathbf{T}_n\, \hat{\mathbf{M}}^{-1}\mathbf{D}_n^+ \left(\hat{\mathbf{\Sigma}}_c^{-1} \otimes \hat{\mathbf{\Sigma}}_c^{-1}\right) \mathbf{D}_n,$$

where $\hat{\mathbf{M}} = \mathbf{D}_n^+[(\hat{\mathbf{C}}_0^\top \otimes \mathbf{I}_n) + (\mathbf{I}_n \otimes \hat{\mathbf{C}}_0^\top)\mathbf{K}_{nn}]\mathbf{T}_n$, $\mathbf{H}_k = \boldsymbol{\eta}_k\boldsymbol{\eta}_k^\top$ (where $\boldsymbol{\eta}_k$ is the k-th canonical basis vector of $\mathbb{R}^n$), $\mathbf{L}_n^s$ is the strict elimination matrix selecting only the below-diagonal elements, $\mathbf{T}_n$ is the lower triangular selection matrix, and $\mathbf{D}_n$, $\mathbf{D}_n^+$, $\mathbf{K}_{nn}$ are the duplication matrix, its Moore–Penrose inverse, and the commutation matrix, respectively.

Proof. See Appendix B. □

Applying the delta method, the asymptotic distribution of the structural parameters is given by

$$\sqrt{T-1}\left(\text{vecl}(\hat{\mathbf{Q}}^{-\top}) - \text{vecl}(\mathbf{Q}^{-\top})\right) \xrightarrow{d} \mathcal{N}\left(\mathbf{0},\ \mathbf{J}\,\mathbf{V}_{\mathbf{\Sigma}_c}\,\mathbf{J}^\top\right), \tag{15}$$

where $\mathbf{V}_{\mathbf{\Sigma}_c}$ is the asymptotic covariance matrix of the MLE estimator of the $n(n+1)/2$ singular elements of $\mathbf{\Sigma}_c$.

2.3 Structural impulse response functions

Our approach computes structural impulse response functions (IRFs) using an explicit structural decomposition, in contrast to Chen et al. (2021). In fact, in our SMAR model

[1] As a robust alternative to ensure validity in finite samples, standard errors can also be obtained through a residual-based bootstrap procedure, which accounts for the potential non-normality of the innovations $\mathbf{E}_t$.

the reduced-form errors ($\mathbf{E}_t$) are generated by a set of underlying uncorrelated structural shocks ($\mathbf{U}_t$) and the link is provided by the structural error in Equation (4). Once we identify $\mathbf{C}_0$, we obtain the orthogonal shocks and thus can trace their causal impact through the IRFs. The orthogonalization is thus performed on the column-wise relationships, as captured by the matrix $\mathbf{C}_0$.

To compute the IRFs, for the sake of simplicity, we consider the vectorized form of a stable MAR(1) model

$$\mathbf{y}_t = \mathbf{\Phi}_1 \mathbf{y}_{t-1} + \mathbf{e}_t,$$

where $\mathbf{y}_t = \text{vec}(\mathbf{Y}_t)$, $\mathbf{\Phi}_1 = (\mathbf{B}_1 \otimes \mathbf{A}_1)$ are the $mn \times mn$ coefficient matrices, $\mathbf{e}_t = \text{vec}(\mathbf{E}_t)$ is the $mn \times 1$ vector of reduced-form errors. The Wold representation of this model is given by

$$\mathbf{y}_t = \sum_{h=0}^{\infty} \mathbf{\Psi}_h \mathbf{e}_{t-h}, \tag{16}$$

where each $mn \times mn$ matrix $\mathbf{\Psi}_h$ represent the h-th impulse response of $\mathbf{y}_t$ to the reduced-form shocks $\mathbf{e}_t$. These matrices can be computed recursively (Lütkepohl, 1990), with $\mathbf{\Psi}_0 = \mathbf{I}_{mn}$, and

$$\mathbf{\Psi}_h = \mathbf{\Phi}_1^h = (\mathbf{B}_1 \otimes \mathbf{A}_1)^h = (\mathbf{B}_1^h \otimes \mathbf{A}_1^h) \qquad \text{for } h \geq 1.$$

In the SMAR model, we have that $\mathbf{E}_t = \mathbf{R}_0^{-1} \mathbf{U}_t \mathbf{C}_0^{-\top}$, which in vectorized form becomes

$$\mathbf{e}_t = \text{vec}(\mathbf{R}_0^{-1} \mathbf{U}_t \mathbf{C}_0^{-\top}) = \left[\mathbf{C}_0^{-1} \otimes \mathbf{R}_0^{-1}\right] \mathbf{u}_t,$$

where $\mathbf{u}_t = \text{vec}(\mathbf{U}_t)$. Let $\mathbf{S} = \left[\mathbf{C}_0^{-1} \otimes \mathbf{R}_0^{-1}\right]$ be the matrix that maps the structural shocks to the reduced-form shocks. Substituting it in Equation (16), yields

$$\mathbf{y}_t = \sum_{h=0}^{\infty} \mathbf{\Psi}_h (\mathbf{S}\mathbf{u}_{t-h}) = \sum_{h=0}^{\infty} (\mathbf{\Psi}_h \mathbf{S}) \mathbf{u}_{t-h}.$$

The structural impulse response coefficient denotes the response of $y_{i,t+h}$ to a unit shock in $u_{j,t}$ which, from the MA version of the vectorized MAR in Equation (16), is equal to

$$\frac{\partial y_{i,t+h}}{\partial u_{j,t}} = \boldsymbol{\eta}_i^{\top} \left(\mathbf{\Psi}_h \mathbf{S}\right) \boldsymbol{\eta}_j,$$

where $\boldsymbol{\eta}_i$ and $\boldsymbol{\eta}_j$ represent the i-th and j-th columns of the identity matrix $\mathbf{I}_{mn}$. Since we imposed $\mathbf{R}_0 = \mathbf{I}_m$, in our model we have $\mathbf{S} = \mathbf{C}_0^{-1} \otimes \mathbf{I}_m$.

To compute the confidence intervals of the structural IRFs, we employ a residual bootstrap procedure (Lütkepohl, 1990; Kilian, 1998). Let $\hat{\mathbf{E}}_t = \mathbf{Y}_t - \hat{\mathbf{A}}_1 \mathbf{Y}_{t-1} \hat{\mathbf{B}}_1^\top$ denote the matrix of reduced-form residuals obtained from the estimated SMAR model, and let $\hat{\mathbf{C}}_0$ be the corresponding structural matrix, we obtain a bootstrap sequence of innovations $\{\mathbf{E}_t^*\}_{t=1}^T$ by resampling from $\{\hat{\mathbf{E}}_t\}$ with replacement. Then, a bootstrap time series $\{\mathbf{Y}_t^*\}_{t=1}^T$ is generated recursively using the estimated matrices of parameters as follows:

$$\mathbf{Y}_t^* = \hat{\mathbf{A}}_1 \mathbf{Y}_{t-1}^* \hat{\mathbf{B}}_1^\top + \mathbf{E}_t^*, \tag{17}$$

initializing at $\mathbf{Y}_0^* = \mathbf{Y}_0$. The SMAR model is then re-estimated on $\{\mathbf{Y}_t^*\}_{t=1}^T$ to obtain bootstrap estimates $\hat{\mathbf{A}}_{1,i}^*$, $\hat{\mathbf{B}}_{1,i}^*$, and $\hat{\mathbf{C}}_0^*$, from which the corresponding structural IRFs, $\boldsymbol{\Theta}_h^* = \boldsymbol{\Psi}_h^* \mathbf{S}^*$, are computed as in Equation (16). Repeating this procedure V times yields the bootstrap distribution $\{\boldsymbol{\Theta}_h^{*(\nu)}\}_{\nu=1}^V$, from which pointwise $(1-\alpha)$ confidence bands at horizon h are constructed as the empirical $\alpha/2$ and $1-\alpha/2$ quantiles (Hall, 1992).

Since each asset i enters the Kronecker structure symmetrically and we do not impose heterogeneous restrictions across assets in $\mathbf{R}_0 = \mathbf{I}_m$, we report the cross-sectional average of the structural IRF for each variable pair $(j \to k)$:

$$\bar{\theta}_{jk,h} = \frac{1}{m} \sum_{i=1}^{m} \boldsymbol{\eta}_{(k-1)m+i}^\top \left(\boldsymbol{\Psi}_h \mathbf{S}\right) \boldsymbol{\eta}_{(j-1)m+i}, \tag{18}$$

where the index $(k-1)m+i$ selects asset i of variable k in the $\mathrm{vec}(\mathbf{Y}_t)$ ordering. Averaging across assets exploits the panel dimension of the data and yields a parsimonious summary of the common propagation mechanism shared by the m assets.

3 SMAR model for returns, volatilities and volumes

In this section, we present the structural form, *i.e.*, the constraints on the $\mathbf{C}_0$ matrix in our model. Although the relationship between trading volumes, volatility, and returns is often complex and context-dependent, the structure of $\mathbf{C}_0$ is imposed by combining financial theory and empirical evidence. First, we refer to the Efficient Market Hypothesis (Fama, 1970), which postulates that asset prices rapidly incorporate all available information, thus making financial returns unpredictable. Second, we consider the MDH, which establishes that both trading volume and volatility are influenced by a latent factor that typically corresponds to the flow of new information arriving in the market. Therefore, when new information becomes available, market participants tend to increase their trading activity, which often results in greater price fluctuations. However, return shocks have an immediate impact on both volatility and volume. Conversely, simultaneous changes in volatility or trading volume are very unlikely to influence returns within the same period (Whitelaw, 1994).

Despite trading volume and volatility generally exhibit a positive correlation, the direction of causality is likely mixed. Some studies suggest that increased trading activity increases volatility, demonstrating that volume acts as a proxy for information inflow (see, among others, Harris, 1987; Lamoureux and Lastrapes, 1990; LeBaron, 1992). In reality, the relationship is likely bidirectional, with feedback effects reinforcing both variables. The MDH (Tauchen and Pitts, 1983) explains that a new flow of information can simultaneously trigger a shock to price dispersion and trading activity. Empirical evidence consistently supports this mechanism across different markets and sample periods (Karpoff, 1987; Gallant et al., 1992; Andersen, 1996). Based on this hypothesis, we choose to treat volume as the most endogenous variable, since it simultaneously responds to return shocks through leverage (Black, 1976; Christie, 1982) and reacts to volatility shocks through the MDH

channel. This shock structure (from asset returns to volatility and then to trading volume) is consistent with the idea that information shocks first influence prices, then generate a reassessment of risk reflected in volatility, and finally influence trading activity (Lamoureux and Lastrapes, 1990; Bessembinder and Seguin, 1993).

To exemplify the structural representation, we discuss a two-asset case in which the matrix of time series is

$$\mathbf{Y}_t = \begin{bmatrix} \log \text{VOL}_{1,t} & \log \text{RBP}_{1,t} & \text{RET}_{1,t} \\ \log \text{VOL}_{2,t} & \log \text{RBP}_{2,t} & \text{RET}_{2,t} \end{bmatrix}, \tag{19}$$

where $\text{VOL}_{i,t}$ is the trading volume of asset i at time t. $\text{RBP}_{i,t}$ is the bipower variation of asset i at time t:

$$\text{RBP}_{i,t} = \frac{\pi}{2} \sum_{\tau=1}^{N_t - 1} |r_{i,\tau}| \cdot |r_{i,\tau+1}|$$

where $r_{i,\tau}$ being the τ-th intraday return of asset i, and N_t is the number of intraday observations on the t-th day, that we use as a proxy for volatility. In addition, daily returns are standardized through a GARCH(1,1) model as follows:

$$\text{RET}_{i,t} = \frac{\Delta \log p_{i,t}}{\hat{\sigma}_{i,t}}$$

where $p_{i,t}$ is the t-th price of asset i and $\hat{\sigma}_{i,t}$ is the conditional volatility estimated with the GARCH(1,1) model.

Given that the matrix $\mathbf{C}_0$ is an upper triangular (Kilian and Lüktepohl, 2017), we normalize the effect of the structural shocks on the errors of the reduced-form model by introducing the column-normalized lower triangular matrix

$$\mathbf{Q}^{-\top} = \mathbf{C}_0^{-\top} \langle \mathbf{C}_0 \rangle = \begin{bmatrix} 1 & 0 & 0 \\ c_{21} & 1 & 0 \\ c_{31} & c_{32} & 1 \end{bmatrix},$$

and the row-normalized triangular matrix

$$\mathbf{W}^{-1} = \langle \mathbf{R}_0 \rangle \mathbf{R}_0^{-1} = \begin{bmatrix} 1 & 0 \\ \rho_{21} & 1 \end{bmatrix},$$

where $\langle \hat{\mathbf{R}}_0 \rangle = \text{diag}(\mathbf{R}_0)$. It follows that the error of the model in Equation (3) can be computed as

$$\mathbf{E}_t = \mathbf{R}_0^{-1} \mathbf{U}_t \mathbf{C}_0^{-\top} = \langle \mathbf{R}_0 \rangle^{-1} \mathbf{W}^{-1} \mathbf{U}_t \mathbf{Q}^{-\top} \langle \mathbf{C}_0 \rangle^{-1},$$

that is

$$\begin{bmatrix} e_{1,t}^{\text{VOL}} & e_{1,t}^{\text{RBP}} & e_{1,t}^{\text{RET}} \\ e_{2,t}^{\text{VOL}} & e_{2,t}^{\text{RBP}} & e_{2,t}^{\text{RET}} \end{bmatrix} = \langle \mathbf{R}_0 \rangle^{-1} \begin{bmatrix} 1 & 0 \\ \rho_{21} & 1 \end{bmatrix} \begin{bmatrix} u_{1,t}^{\text{VOL}} & u_{1,t}^{\text{RBP}} & u_{1,t}^{\text{RET}} \\ u_{2,t}^{\text{VOL}} & u_{2,t}^{\text{RBP}} & u_{2,t}^{\text{RET}} \end{bmatrix} \begin{bmatrix} 1 & 0 & 0 \\ c_{21} & 1 & 0 \\ c_{31} & c_{32} & 1 \end{bmatrix} \langle \mathbf{C}_0 \rangle^{-1}.$$

Defining $\tilde{\mathbf{E}}_t = \mathbf{W}^{-1} \mathbf{U}_t \mathbf{Q}^{-\top}$, which are the standardized errors of the reduced-form model, we get

$$\begin{aligned} \tilde{e}_{1,t}^{\text{VOL}} &= u_{1,t}^{\text{VOL}} + u_{1,t}^{\text{RBP}} c_{21} + u_{1,t}^{\text{RET}} c_{31} \\ \tilde{e}_{1,t}^{\text{RBP}} &= u_{1,t}^{\text{RBP}} + u_{1,t}^{\text{RET}} c_{32} \\ \tilde{e}_{1,t}^{\text{RET}} &= u_{1,t}^{\text{RET}} \end{aligned}$$

for the first row of $\tilde{\mathbf{E}}_t$, and

$$\begin{aligned} \tilde{e}_{2,t}^{\text{VOL}} &= (\rho_{21} u_{1,t}^{\text{VOL}} + u_{2,t}^{\text{VOL}}) + (\rho_{21} u_{1,t}^{\text{RBP}} + u_{2,t}^{\text{RBP}}) c_{21} + (\rho_{21} u_{1,t}^{\text{RET}} + u_{2,t}^{\text{RET}}) c_{31} \\ \tilde{e}_{2,t}^{\text{RBP}} &= (\rho_{21} u_{1,t}^{\text{RBP}} + u_{2,t}^{\text{RBP}}) + (\rho_{21} u_{1,t}^{\text{RET}} + u_{2,t}^{\text{RET}}) c_{32} \\ \tilde{e}_{2,t}^{\text{RET}} &= \rho_{21} u_{1,t}^{\text{RET}} + u_{2,t}^{\text{RET}} \end{aligned} \tag{20}$$

for the second row of $\tilde{\mathbf{E}}_t$.

This decomposition highlights the explanatory power of the model. Indeed, the error equations for the first asset (the n-dimensional vector $\tilde{\mathbf{e}}_{1,t}$) show how structural shocks to a financial variable simultaneously impact other variables within the same asset. The

parameters c_{ij} quantify the magnitude of these effects across variables within the same asset.

The error equations for the second asset ($\tilde{\mathbf{e}}_{2,t}$) concern contagion between assets. The parameter ρ_{21} governs the extent to which structural shocks originating in asset 1 are transmitted to asset 2. For example, the term $\rho_{21}u_{1,t}^{\text{RET}} + u_{2,t}^{\text{RET}}$ represents the total return shock affecting asset 2, which is a combination of its shock and the portion spilling over from asset 1. As already stated at the end of Section 2.1, we set $\mathbf{R}_0 = \mathbf{I}_m$ to avoid any contagion effect between all assets. Analytically, the system (20) reduces to

$$\begin{aligned}
\tilde{e}_{2,t}^{\text{VOL}} &= u_{2,t}^{\text{VOL}} + u_{2,t}^{\text{RBP}} c_{21} + u_{2,t}^{\text{RET}} c_{31} \\
\tilde{e}_{2,t}^{\text{RBP}} &= u_{2,t}^{\text{RBP}} + u_{2,t}^{\text{RET}} c_{32} \\
\tilde{e}_{2,t}^{\text{RET}} &= u_{2,t}^{\text{RET}}.
\end{aligned} \tag{21}$$

4 Empirical analysis

Our sample consists of the daily prices and volumes of the assets comprising the Dow Jones Industrial Average (as of April 2025), collected between January 2021 and February 2025 ($T = 1059$ observations). The data are sourced from Bloomberg. The variables used in the analysis are computed as shown in Section 3. Moreover, to avoid estimating the constant-value matrix[2], all series are standardized. Based on the results of the Bayesian Information Criterion (BIC), we specify a SMAR(1).

As further detailed in Section 2.2, the reduced-form MAR(1) defined as in Equation (3) is estimated via maximum likelihood. The model is stationary since the product of the spectral radii is $\rho(\hat{\mathbf{A}}_1)\,\rho(\hat{\mathbf{B}}_1) \approx 0.989$ (see Chen et al., 2021). Equation (22) reports the

[2]Through a preliminary analysis (available upon request from the authors) of the time series, we noted that the inclusion of a constant in the SMAR model can generate collinearity problems for a large number of assets, and can often lead to the estimation of singular matrices. This also affects the estimation time, which becomes increasingly longer as m increases.

estimated $\hat{\mathbf{B}}_1$, with corresponding standard errors provided in parentheses and bold values indicating a 5% significance:

$$\hat{\mathbf{B}}_1 = \begin{bmatrix} \underset{(0.0199)}{\mathbf{3.5765}} & \underset{(0.0159)}{\mathbf{-0.3975}} & \underset{(0.0114)}{\mathbf{-0.0460}} \\ \underset{(0.0118)}{\mathbf{0.6307}} & \underset{(0.0155)}{\mathbf{1.9885}} & \underset{(0.0105)}{0.0072} \\ \underset{(0.0146)}{0.0188} & \underset{(0.0180)}{-0.0122} & \underset{(0.0142)}{0.0041} \end{bmatrix}. \tag{22}$$

For instance, the first column shows the impact on financial variables from past volumes. Consistently with the literature on volatility clustering and long-memory properties in market activity, both trading volume and volatility exhibit a high degree of persistence. We also observe a significant cross-variable feedback between volume and volatility. Specifically, past trading volume has a positive and significant impact on current volatility, supporting the idea that intense activity anticipates higher price dispersion. Conversely, past volatility has a significant effect on current volume, suggesting a potential "cooling off" effect in trading activity following periods of high uncertainty. Finally, the coefficients related to lagged returns in the equations for volume and volatility are relatively small, although the negative impact on volume is statistically significant. This somehow provides evidence of asymmetric dynamics, where past price movements slightly influence market participation. In line with the efficient market hypothesis discussed in Section 2.1, asset returns appear to be largely independent of the lagged values of all variables.

Then, using the estimated covariance matrix $\hat{\mathbf{\Sigma}}_{\mathrm{c}}$, we derive the inverse of the contemporaneous column-wise matrix with normalized diagonal, $\hat{\mathbf{Q}}^{-\top}$, which takes the following values (with standard errors reported in parentheses and bold values indicating a 5% significance):

$$\hat{\mathbf{Q}}^{-\top} = \begin{bmatrix} 1.0000 & 0.0000 & 0.0000 \\ \underset{(0.0051)}{\mathbf{0.5075}} & 1.0000 & 0.0000 \\ \underset{(0.0024)}{\mathbf{-0.0460}} & \underset{(0.0020)}{\mathbf{-0.0473}} & 1.0000 \end{bmatrix}. \tag{23}$$

The interpretation of the estimated inverse of $\hat{\mathbf{Q}}^\top$ in Equation (23) provides a clear and economically significant causal ordering. The highest coefficient is 0.5075, which indicates that a one-standard-deviation structural shock to market volatility (RBP) leads to a strong, significant, and immediate positive response in trading volumes. This finding suggests that unexpected changes in market uncertainty are a primary driver of contemporaneous trading activity, as market participants rapidly adjust their positions in response.

Furthermore, we find that a structural shock to returns has a negative impact on both trading volume (-0.0460) and volatility (-0.0473). This is consistent with the leverage effect (Black, 1976): negative return shocks are associated with an immediate increase in perceived risk. The nearly equal magnitude of the two coefficients suggests that the information content of the return shocks is transmitted symmetrically to the other variables, rather than being absorbed first by one and then by the other. Notably, both effects are small relative to the volatility-volume coefficient (0.5075), reinforcing the view that uncertainty about future prices, rather than the return itself, is the dominant contemporaneous driver of trading activity.

Then, we analyze the average inverse response functions in Figure 1. Looking at the diagonal (*i.e.*, self-responses to a shock), it can be noticed that the self-response to a shock in returns tends to zero immediately after one lag. This is in large part coherent with the theory of market efficiency by Fama (1970). Conversely, both the self-responses of volume and RBP decay slowly, consistent with the volatility clustering theory (Engle, 1982; Andersen et al., 2001) and long-memory of the trading volume (Bessembinder and Seguin, 1993; Lobato and Velasco, 2000).

Interestingly, a shock in the realized bipower leads to an immediate and persistent increase in the volume. This finding confirms what is stated in the MDH: news arrives and simultaneously moves prices and volumes. When we analyze the opposite direction (*i.e.*, the effect of a shock in the volumes on RBP), it emerges that the increase in the volatility

Figure 1: Average structural impulse response function

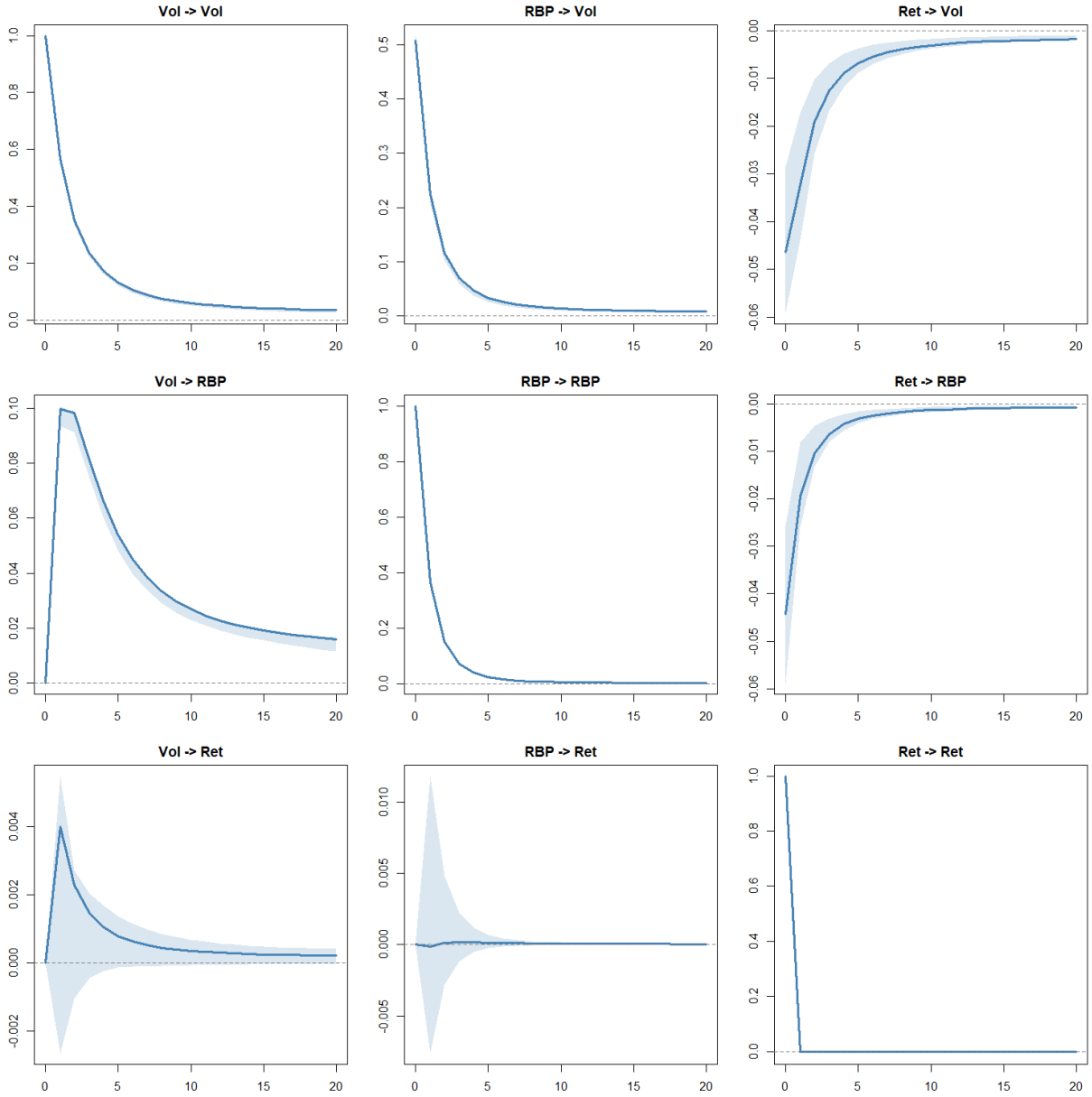

Note: The light blue area represents the 90% bootstrapped confidence interval on 200 replicates. The first variable is the one shocked, while the second one is the response.

is slightly lagged. Therefore, the intense trading activity precedes or feeds the dispersion in prices in the following periods. It should be further noticed that the magnitude of the response of trading volume to a shock in RBP is markedly different from the opposite. This implies market participants massively react increasing their trading activity when prices start fluctuating. In other words, volatility generates uncertainty, thus it forces buyers and sellers to immediately adjust their investment strategies. In addition, we find that the effect of a shock in the volumes on volatility is much more persistent than the opposite. This asymmetry in persistence constitutes, to our knowledge, a novel finding in the structural analysis of the volume–volatility nexus.

The existing literature has primarily documented the contemporaneous and short-run relationship between volumes and volatility. Gallant et al. (1992), using a semi-nonparametric bivariate framework, provide impulse response profiles for stock prices and volume and document that volume reacts strongly to price innovations, but do not examine the dynamic propagation between trading volume and volatility, nor distinguish the persistence of shocks across these two variables. Tauchen and Pitts (1983) and Andersen (1996) focus on the contemporaneous co-movement implied by the latent information flow under the MDH, without characterizing the differential decay of cross-variable impulse responses at medium horizons. Bollerslev and Jubinski (1999), examining the common fractional integration and long-run dependence between volume and volatility, find that both variables share a common fractionally integrated component driven by information arrival, but their framework abstracts from the short-to-medium-run asymmetry in impulse propagation that we document here.

The key contribution of our structural identification is that, by orthogonalizing shocks via $\hat{\mathbf{C}}_0$, we can isolate the dynamic effect of structural volume innovations on volatility. The resulting persistence is consistent with market microstructure models in which information is incorporated gradually through order flow (Kyle, 1985), implying that the

impact of trading activity on price variability unfolds over several trading days rather than instantaneously.

4.1 Decomposition of Trading Volume Variance

One of the aims of this paper is to disentangle the component of trading volume driven by informational shocks from that attributable to liquidity dynamics. The structural framework introduced in Section 2 makes this decomposition possible through the forecast error variance decomposition (FEVD) of the model.

Since the SMAR operates on an $m \times n$ data matrix time series, the forecast error variance of trading volume for any given asset i receives contributions from two distinct sources: shocks originating within the same asset (column-wise effects, governed by $\mathbf{C}_0$) and shocks originating in other assets (row-wise effects, transmitted through the lagged dynamics of $\hat{\mathbf{A}}_1$). We refer to these as the within-asset and cross-asset components, respectively.

Formally, we derive the FEVD from the structural moving average representation established in Section 2.3. Recall that the vectorized SMAR admits the representation

$$\mathbf{y}_t = \sum_{l=0}^{\infty} \boldsymbol{\Theta}_l \, \mathbf{u}_{t-l}, \qquad \boldsymbol{\Theta}_l \equiv \boldsymbol{\Psi}_l \mathbf{S}, \tag{24}$$

where $\mathbf{S} = \left[\mathbf{C}_0^{-1} \otimes \mathbf{I}_m\right]$ (using $\mathbf{R}_0 = \mathbf{I}_m$), $\mathbf{u}_t = \mathrm{vec}(\mathbf{U}_t)$ is the $mn \times 1$ vector of structural shocks with $\boldsymbol{\Omega} = \mathrm{Var}(\mathbf{u}_t) = \mathbf{I}_{mn}$ (see Equation (2)), and the $mn \times mn$ matrices $\boldsymbol{\Psi}_l$ are the reduced-form impulse responses computed recursively as in Section 2.3.

The h-step-ahead forecast error (Lütkepohl, 2005), conditional on information at time t, is

$$\boldsymbol{\xi}_{t+h|t} \equiv \mathbf{y}_{t+h} - \mathbb{E}_t[\mathbf{y}_{t+h}] = \sum_{l=0}^{h-1} \boldsymbol{\Theta}_l \, \mathbf{u}_{t+h-l}. \tag{25}$$

Let $\iota_{ik} \equiv (k-1)m + i$ denote the index of variable k of asset i in $\mathbf{y}_t$, and let $\boldsymbol{\eta}_s$ denote the s-th column of $\mathbf{I}_{mn}$, so that $\boldsymbol{\eta}_{\iota_{ik}}^{\top} \mathbf{y}_t$ selects the element corresponding to variable k of asset i. Since the structural shocks are mutually uncorrelated with unit variance, the h-step

forecast error variance of variable k for asset i is

$$\mathcal{V}_{ik}(h) \equiv \mathrm{Var}\big(\boldsymbol{\eta}_{\iota_{ik}}^{\top}\,\boldsymbol{\xi}_{t+h|t}\big) = \boldsymbol{\eta}_{\iota_{ik}}^{\top}\left(\sum_{l=0}^{h-1}\boldsymbol{\Theta}_l\,\mathbf{I}_{mn}\,\boldsymbol{\Theta}_l^{\top}\right)\boldsymbol{\eta}_{\iota_{ik}}$$
$$= \sum_{l=0}^{h-1}\boldsymbol{\eta}_{\iota_{ik}}^{\top}\boldsymbol{\Theta}_l\boldsymbol{\Theta}_l^{\top}\boldsymbol{\eta}_{\iota_{ik}}. \tag{26}$$

Since $\boldsymbol{\eta}_{\iota_{ik}}^{\top}\boldsymbol{\Theta}_l\boldsymbol{\Theta}_l^{\top}\boldsymbol{\eta}_{\iota_{ik}} = \left\|\boldsymbol{\eta}_{\iota_{ik}}^{\top}\boldsymbol{\Theta}_l\right\|^2 = \sum_{s=1}^{mn}\left[\boldsymbol{\eta}_{\iota_{ik}}^{\top}\boldsymbol{\Theta}_l\,\boldsymbol{\eta}_s\right]^2$, Equation (26) can be written as

$$\mathcal{V}_{ik}(h) = \sum_{l=0}^{h-1}\sum_{s=1}^{mn}\left[\boldsymbol{\eta}_{\iota_{ik}}^{\top}\boldsymbol{\Theta}_l\,\boldsymbol{\eta}_s\right]^2, \tag{27}$$

where each term $\left[\boldsymbol{\eta}_{\iota_{ik}}^{\top}\boldsymbol{\Theta}_l\,\boldsymbol{\eta}_s\right]^2$ represents the squared structural impulse response at horizon l. Because the mn structural shocks are orthogonal (*i.e.*, $\boldsymbol{\Omega} = \mathbf{I}_{mn}$), the total variance decomposes additively (Lütkepohl, 2005; Kilian and Lüktepohl, 2017). Denoting the contribution of the s-th structural shock as

$$\mathcal{V}_{ik}^{(s)}(h) \equiv \sum_{l=0}^{h-1}\left[\boldsymbol{\eta}_{\iota_{ik}}^{\top}\boldsymbol{\Theta}_l\,\boldsymbol{\eta}_s\right]^2, \tag{28}$$

it follows immediately from (27) that

$$\sum_{s=1}^{mn}\mathcal{V}_{ik}^{(s)}(h) = \mathcal{V}_{ik}(h).$$

In $\mathbf{u}_t$, the structural shocks originating from asset i occupy the n positions $\{(j-1)m+i\colon j=1,\ldots,n\}$, corresponding to the three financial variables (VOL, RBP, RET) of that asset. Summing over these positions gives the within-asset component

$$\mathcal{V}_{ik}^{\text{within}}(h) = \sum_{j=1}^{n}\mathcal{V}_{ik}^{((j-1)m+i)}(h) = \sum_{j=1}^{n}\sum_{l=0}^{h-1}\left[\boldsymbol{\eta}_{\iota_{ik}}^{\top}\boldsymbol{\Theta}_l\,\boldsymbol{\eta}_{(j-1)m+i}\right]^2, \tag{29}$$

which we denote $\mathcal{V}_{ik}^{j}(h) \equiv \mathcal{V}_{ik}^{((j-1)m+i)}(h)$ for $j \in \{1,\ldots,n\}$. The cross-asset component collects all remaining shock contributions and is obtained by difference

$$\mathcal{V}_{ik}^{\text{cross}}(h) = \mathcal{V}_{ik}(h) - \mathcal{V}_{ik}^{\text{within}}(h) = \sum_{\substack{s=1 \\ s\notin\{(j-1)m+i\}_{j=1}^{n}}}^{mn}\mathcal{V}_{ik}^{(s)}(h). \tag{30}$$

Normalising by the total variance and averaging across the m assets yields

$$\overline{\text{FEVD}}_{jk}(h) = \frac{\frac{1}{m}\sum_{i=1}^{m} \mathcal{V}_{ik}^{j}(h)}{\frac{1}{m}\sum_{i=1}^{m} \mathcal{V}_{ik}(h)}, \qquad j \in \{\text{VOL, RBP, RET}\}, \tag{31}$$

and analogously for the cross-asset share

$$\overline{\text{FEVD}}_{\text{cross},k}(h) = \frac{\frac{1}{m}\sum_{i=1}^{m} \mathcal{V}_{ik}^{\text{cross}}(h)}{\frac{1}{m}\sum_{i=1}^{m} \mathcal{V}_{ik}(h)}. \tag{32}$$

By construction,$\overline{\text{FEVD}}_{\text{VOL},k}(h) + \overline{\text{FEVD}}_{\text{RBP},k}(h) + \overline{\text{FEVD}}_{\text{RET},k}(h) + \overline{\text{FEVD}}_{\text{cross},k}(h) = 1$ at every horizon h. At $h = 1$, since $\mathbf{R}_0 = \mathbf{I}_m$ rules out any contemporaneous cross-asset transmission, $\overline{\text{FEVD}}_{\text{cross},k}(1) = 0$ exactly and the three within-asset components account for the full variance. As the horizon grows, cross-asset contributions accumulate through the lagged dynamics encoded in $\hat{\mathbf{A}}_1$.

We label $\overline{\text{FEVD}}_{\text{RBP},k}$ as the *informative component* of trading volume, since it captures the fraction of trading activity driven by the latent information flow that simultaneously moves prices and volumes under the MDH (Tauchen and Pitts, 1983). Conversely, $\overline{\text{FEVD}}_{\text{VOL},k}$ constitutes the *liquidity component*, reflecting trading activity unrelated to contemporaneous changes in price dispersion.

Table 1 reports the four components for trading volume ($k = \text{VOL}$) at horizons $h \in \{1, 5, 10, 20\}$. At the impact horizon ($h = 1$), approximately 20.4% of volume variance is attributable to the RBP shock and 79.4% to the volume's own shock, confirming that same-day trading activity is dominated by asset-specific liquidity dynamics with a non-trivial informational contribution. The return shock accounts for a negligible 0.2%, reflecting the near-zero contemporaneous effect of returns on volume visible in Figure 1.

As the horizon expands, both within-asset components decline in favour of cross-asset spillovers. At $h = 20$, cross-asset dynamics explain 56.9% of total volume variance, while

Table 1: Average FEVD of trading volume (%)

Shock	$h = 1$	$h = 5$	$h = 10$	$h = 20$
RBP_t (informative)	20.4	13.1	9.9	7.2
VOL_t (liquidity)	79.4	61.8	47.9	35.8
RET_t	0.2	0.1	0.1	0.1
Cross-Asset Spillovers	0.0	25.0	42.1	56.9

the informative and liquidity components decline to 7.2% and 35.8%, respectively. This decrease reflects the high integration of the Dow Jones constituents: after the initial within-asset response, volatility and liquidity shocks in one stock propagate to others through the estimated $\hat{\mathbf{A}}_1$ matrix, generating system-wide co-movement in trading activity that dwarfs the asset-level components at medium and long horizons. The stacked area chart in Figure 2 visualizes this transition continuously over the 20-day horizon.

4.2 Informative component around FOMC

To further validate our structural identification, we analyze the time series dynamics of the informative component around exogenous information shocks. We define the daily informative share at time t as

$$\widehat{s}_t = \frac{\sum_{i=1}^{m} \left(\hat{c}_{21}\, \hat{u}_{i,t}^{\text{RBP}}\right)^2}{\sum_{i=1}^{m} \left(\tilde{\hat{e}}_{i,t}^{\text{VOL}}\right)^2}, \tag{33}$$

where $\tilde{\hat{e}}_{i,t}^{\text{VOL}}$ is the standardized reduced-form residual for the volume of asset i at day t, $\hat{u}_{i,t}^{\text{RBP}} = \sum_j [\hat{\mathbf{Q}}^\top]_{j,\text{RBP}}\, \tilde{\hat{e}}_{i,j,t}$ is the recovered structural RBP shock obtained by inverting $\tilde{\mathbf{E}}_t = \mathbf{U}_t \mathbf{Q}^{-\top}$, and $\hat{c}_{21}$ is the estimated element of $\mathbf{Q}^{-\top}$ governing the contemporaneous impact of volatility on volume. This sample analog of the FEVD informative component varies daily with the realized residuals and provides a time-varying measure of the information

Figure 2: Stacked FEVD of Trading Volume

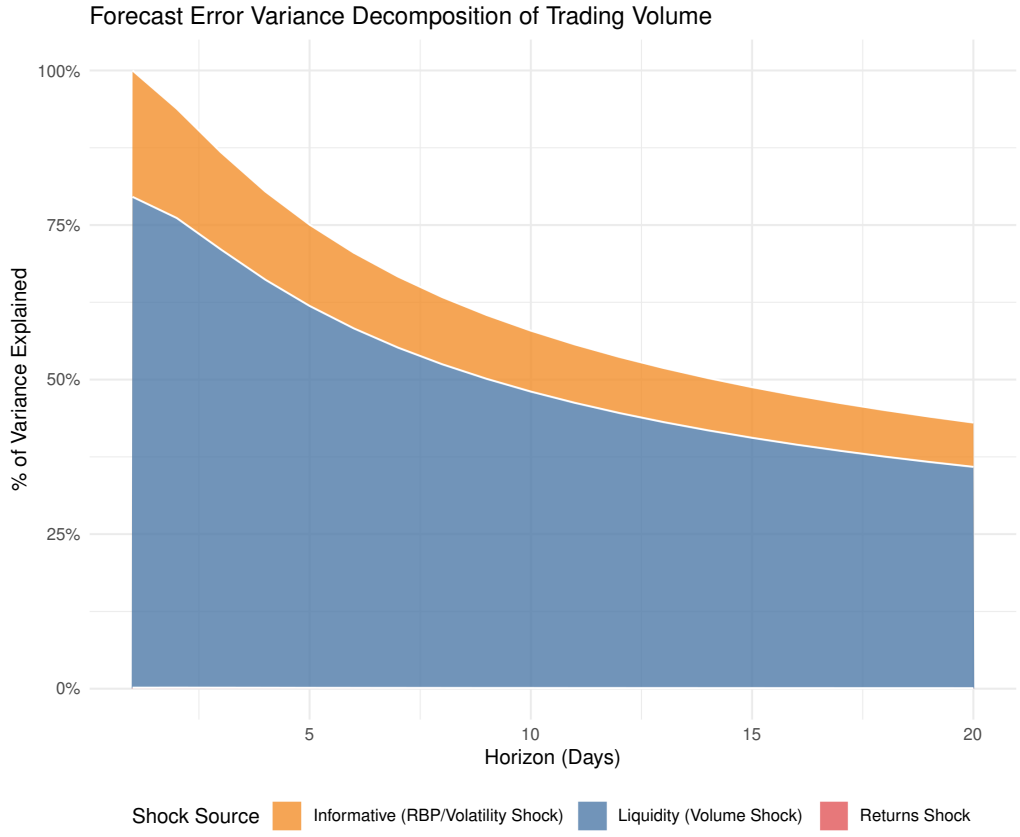

Note: The blue area represents the liquidity component (own-volume shock), the orange area represents the informative component (RBP shock), while the red area identifies the fraction of variance explained by returns. The white space above the colored areas indicates the variance explained by cross-asset spillovers.

content of trading activity.

We then conduct an event study centered on Federal Open Market Committee (FOMC) announcements from 2021 to 2025 (Lucca and Moench, 2015). As shown in Figure 3, the informative share of trading volume remains stable and close to the unconditional mean (dotted line) during the pre-announcement window, followed by a sharp and statistically significant spike exactly on the day of the event ($t = 0$). This immediate reaction confirms that our SMAR-based decomposition effectively isolates volume surges triggered by systematic information arrival. Furthermore, the rapid reversion toward the mean in the

subsequent days $(t+1, t+2)$ suggests that the Dow Jones constituents incorporate macroeconomic news efficiently, validating the RBP-volume channel as a reliable proxy for the latent information flow.

Figure 3: Informative share of volume around FOMC announcements (Validated)

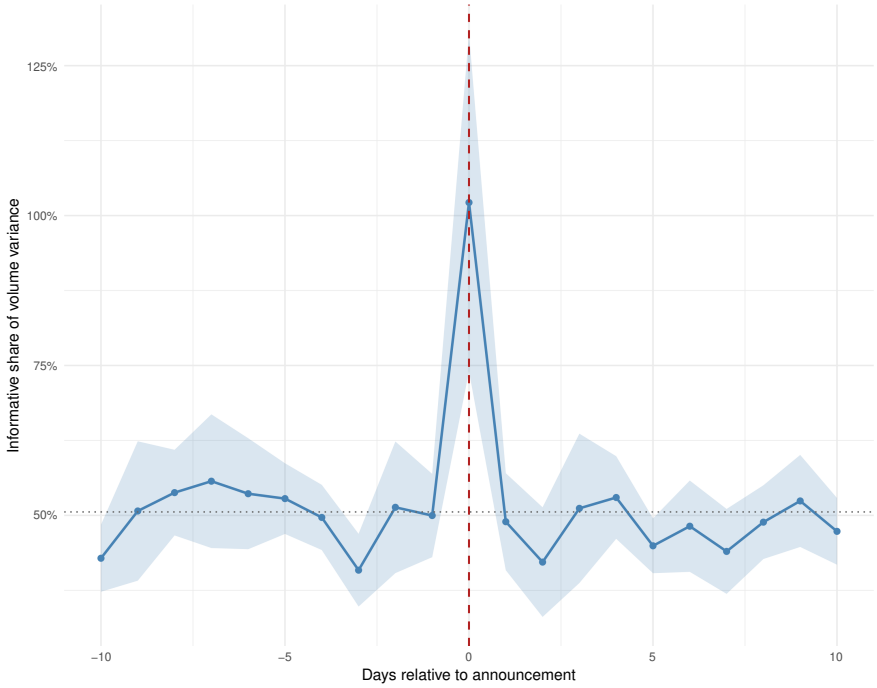

Note: The plot shows the average daily informative share of volume variance across 33 FOMC events. The spike at $t = 0$ denotes the contemporaneous impact of the macro announcement. The dotted line represents the sample mean, and the shaded area indicates the 90% confidence interval.

5 Conclusions

This paper introduces the Structural Matrix Autoregressive (SMAR) model, a flexible framework that jointly accounts for contemporaneous and dynamic interdependencies in high-dimensional financial time series. By extending the MAR model of Chen et al. (2021), the SMAR explicitly incorporates structural relationships between assets and financial variables via two contemporaneous interaction matrices, $\mathbf{C}_0$ and $\mathbf{R}_0$, thereby providing

a tractable identification strategy for orthogonal structural shocks and a natural decomposition of forecast error variance even in large cross-sections.

The identification of the structural matrix $\mathbf{C}_0$ is based on a theory-driven recursive ordering, *i.e.*, returns, realized bipower variance, and trading volume, consistent with the efficient market hypothesis and the mixture-of-distributions hypothesis. The assumption $\mathbf{R}_0 = \mathbf{I}_m$, while tractable, abstracts from contemporaneous cross-asset spillovers and represents a natural departure point for future extensions.

Applied to daily data for the constituents of the Dow Jones Industrial Average from January 2021 to February 2025, the SMAR delivers four main findings. First, the estimated contemporaneous structure confirms that unexpected changes in realized bipower variance are the primary driver of contemporaneous trading activity: a one-standard-deviation volatility shock results in an immediate and economically large increase in volumes, consistent with the MDH. Second, the structural impulse responses reveal a pronounced asymmetry. In fact, while volatility shocks generate a large and rapid volume response, the effect of volume shocks on volatility is comparatively modest at short horizons but markedly more persistent at longer horizons, suggesting that liquidity-driven trading gradually feeds back into price dispersion rather than producing an immediate reassessment of risk. Third, the forecast error variance decomposition shows that at the one-day horizon trading volume is mainly driven by own-liquidity dynamics (79.4%) with a non-trivial informational component (20.4%); as the horizon extends to twenty days, cross-asset spillovers account for over half of total volume variance (56.9%), highlighting the strong integration of Dow Jones constituents. Fourth, an event study around Federal Open Market Committee announcements confirms that the RBP-based informative component spikes sharply and significantly on announcement days and reverts rapidly thereafter.

Despite the promising results of the SMAR, several challenges remain. For instance, the assumption of no contemporaneous cross-asset effects is an oversimplification that could

be relaxed. Future work could explore more complex identification strategies for $\mathbf{R}_0$, *e.g.*, using network theory or factor models. Additionally, the framework could be extended to incorporate time-varying parameters, allowing the model to capture evolving market structures and changing responses to different economic regimes.

References

Acharya, V. V. and Pedersen, L. H. (2005). Asset pricing with liquidity risk. Journal of Financial Economics, 77(2):375–410.

Andersen, T. G. (1996). Return Volatility and Trading Volume: An Information Flow Interpretation of Stochastic Volatility. The Journal of Finance, 51(1):169–204.

Andersen, T. G., Bollerslev, T., Diebold, F. X., and Ebens, H. (2001). The distribution of realized stock return volatility. Journal of Financial Economics, 61(1):43–76.

Andersen, T. G., Bollerslev, T., Diebold, F. X., and Vega, C. (2003). Micro Effects of Macro Announcements: Real-Time Price Discovery in Foreign Exchange. American Economic Review, 93(1):38–62.

Bessembinder, H. and Seguin, P. J. (1993). Price Volatility, Trading Volume, and Market Depth: Evidence from Futures Markets. The Journal of Financial and Quantitative Analysis, 28(1):21–39.

Black, F. (1976). Studies of stock price volatility changes. In Proceedings of the 1976 Meeting of the Business and Economic Statistics Section, American Statistical Association, Washington DC.

Bollerslev, T. and Jubinski, D. (1999). Equity Trading Volume and Volatility: Latent Infor-

mation Arrivals and Common Long-Run Dependencies. Journal of Business & Economic Statistics, 17(1):9–21.

Bollerslev, T., Li, J., and Xue, Y. (2018). Volume, Volatility, and Public News Announcements. The Review of Economic Studies, 85(4):2005–2041.

Brunnermeier, M. K. and Pedersen, L. H. (2009). Market Liquidity and Funding Liquidity. The Review of Financial Studies, 22(6):2201–2238.

Bucci, A., Palomba, G., and Tedeschi, M. (2026). Matrix-valued AutoRegressive (MAR) models in gretl. Computational Statistics, 41:1–47.

Canova, F. and Ciccarelli, M. (2013). Panel vector autoregressive models: a survey. Technical Report 1507, European Central Bank.

Chen, R., Xiao, H., and Yang, D. (2021). Autoregressive models for matrix-valued time series. Journal of Econometrics, 222(1, Part B):539–560.

Chiang, T. C., Qiao, Z., and Wong, W.-K. (2010). New evidence on the relation between return volatility and trading volume. Journal of Forecasting, 29(5):502–515.

Chordia, T., Roll, R., and Subrahmanyam, A. (2000). Commonality in liquidity. Journal of Financial Economics, 56:3–28.

Christie, A. A. (1982). The Stochastic Behavior of Common Stock Variances. Journal of Financial Economics, 10(4):407–432.

Darolles, S., Le Fol, G., and Mero, G. (2015). Measuring the liquidity part of volume. Journal of Banking & Finance, 50:92–105.

Diebold, F. X. and Yilmaz, K. (2009). Measuring Financial Asset Return and Volatility Spillovers, with Application to Global Equity Markets. The Economic Journal, 119(534):158–171.

Dutilleul, P. (1999). The mle algorithm for the matrix normal distribution. Journal of Statistical Computation and Simulation, 64(2):105–123.

Engle, R. F. (1982). Autoregressive Conditional Heteroscedasticity with Estimates of the Variance of United Kingdom Inflation. Econometrica, 50(4):987–1007.

Fama, E. F. (1970). Efficient Capital Markets: A Review of Theory and Empirical Work. The Journal of Finance, 25(2):383–417.

Gallant, A. R., Rossi, P. E., and Tauchen, G. (1992). Stock prices and volume. The Review of Financial Studies, 5(2):199–242.

Hall, P. (1992). The Bootstrap and Edgeworth Expansion. Springer-Verlag.

Harris, L. (1987). Transaction Data Tests of the Mixture of Distributions Hypothesis. The Journal of Financial and Quantitative Analysis, 22(2):127–141.

He, X. and Velu, R. (2014). Volume and Volatility in a Common-Factor Mixture of Distributions Model. The Journal of Financial and Quantitative Analysis, 49(1):33–49.

Herwartz, H. and Wang, S. (2024). Statistical identification in panel structural vector autoregressive models based on independence criteria. Journal of Applied Econometrics, 39(4):620–639.

Karpoff, J. M. (1987). The Relation Between Price Changes and Trading Volume: A Survey. The Journal of Financial and Quantitative Analysis, 22(1):109–126.

Kilian, L. (1998). Small-Sample Confidence Intervals for Impulse Response Functions. The Review of Economics and Statistics, 80(2):218–230.

Kilian, L. and Lüktepohl, H. (2017). Structural Vector Autoregressive Analysis. Cambridge University Press.

Kyle, A. S. (1985). Continuous Auctions and Insider Trading. Econometrica, 53(6):1315–1335.

Lamoureux, C. G. and Lastrapes, W. D. (1990). Heteroskedasticity in stock return data: Volume versus GARCH effects. The Journal of Finance, 45(1):221–229.

LeBaron, B. (1992). Forecast improvements using a volatility index. Journal of Applied Econometrics, 7:S137–S149.

Lobato, I. N. and Velasco, C. (2000). Long Memory in Stock-Market Trading Volume. Journal of Business & Economic Statistics, 18(4):410–427.

Longin, F. and Solnik, B. (2001). Extreme Correlation of International Equity Markets. The Journal of Finance, 56(2):649–676.

Lucca, D. O. and Moench, E. (2015). The Pre-FOMC Announcement Drift. The Journal of Finance, 70(1):329–371.

Lütkepohl, H. (1990). Asymptotic Distributions of Impulse Response Functions and Forecast Error Variance Decompositions of Vector Autoregressive Models. The Review of Economics and Statistics, 72(1):116–125.

Lütkepohl, H. (2005). New Introduction to Multiple Time Series Analysis. Springer Science & Business Media, Berlin, Heidelberg.

Pástor, L. and Stambaugh, R. F. (2003). Liquidity Risk and Expected Stock Returns. Journal of Political Economy, 111(3):642–685.

Sims, C. A. (1980). Macroeconomics and reality. Econometrica, 48(1):1–48.

Tauchen, G. E. and Pitts, M. (1983). The Price Variability-Volume Relationship on Speculative Markets. Econometrica, 51(2):485–505.

Whitelaw, R. F. (1994). Time Variations and Covariations in the Expectation and Volatility of Stock Market Returns. The Journal of Finance, 49(2):515–541.

Wu, F. and Chan, K.-S. (2026). Mixture matrix-valued autoregressive model. Journal of Econometrics, 255:106245.

A Derivation of the score function

We derive the per-observation score $\mathbf{s}_t(\boldsymbol{\beta})$ from the log-likelihood contribution

$$\ell_t = -\frac{m}{2}\log|\boldsymbol{\Sigma}_{\mathrm{c}}| - \frac{n}{2}\log|\boldsymbol{\Sigma}_{\mathrm{r}}| - \frac{1}{2}\operatorname{tr}\big(\boldsymbol{\Sigma}_{\mathrm{r}}^{-1}\mathbf{E}_t\boldsymbol{\Sigma}_{\mathrm{c}}^{-1}\mathbf{E}_t^\top\big)\,,$$

where $\mathbf{E}_t = \mathbf{Y}_t - \mathbf{A}_1\mathbf{Y}_{t-1}\mathbf{B}_1^\top$ is $m\times n$, $\boldsymbol{\Sigma}_{\mathrm{r}}$ is $m\times m$, and $\boldsymbol{\Sigma}_{\mathrm{c}}$ is $n\times n$. We rely on two standard tools throughout. First, the trace inner product: $df = \operatorname{tr}(\mathbf{Z}\,d\mathbf{X})$ identifies $\partial f/\partial\mathbf{X} = \mathbf{Z}^\top$, and equivalently $df = [\operatorname{vec}(\mathbf{Z}^\top)]^\top\operatorname{vec}(d\mathbf{X})$. Second, the duplication matrix $\mathbf{D}_k$ of order k, defined by $\operatorname{vec}(\boldsymbol{\Upsilon}) = \mathbf{D}_k\operatorname{vech}(\boldsymbol{\Upsilon})$ for any symmetric $k\times k$ matrix $\boldsymbol{\Upsilon}$, so that restricting the differential to the symmetric subspace gives $\operatorname{vec}(d\boldsymbol{\Upsilon}) = \mathbf{D}_k\,d\operatorname{vech}(\boldsymbol{\Upsilon})$, and therefore $\partial f/\partial\operatorname{vech}(\boldsymbol{\Upsilon}) = \mathbf{D}_k^\top\operatorname{vec}(\partial f/\partial\boldsymbol{\Upsilon})$.

A.1 Score with respect to $\operatorname{vec}(\mathbf{A}_1)$

Taking the differential of the quadratic term with $d\mathbf{E}_t = -(d\mathbf{A}_1)\mathbf{Y}_{t-1}\mathbf{B}_1^\top$ gives the following

$$d\ell_t = -\frac{1}{2}\operatorname{tr}\big(\boldsymbol{\Sigma}_{\mathrm{r}}^{-1}d\mathbf{E}_t\,\boldsymbol{\Sigma}_{\mathrm{c}}^{-1}\mathbf{E}_t^\top\big) - \frac{1}{2}\operatorname{tr}\big(\boldsymbol{\Sigma}_{\mathrm{r}}^{-1}\mathbf{E}_t\,\boldsymbol{\Sigma}_{\mathrm{c}}^{-1}d\mathbf{E}_t^\top\big)\,.$$

Because the two terms are transposes of each other inside the trace, they are equal, so

$$d\ell_t = \operatorname{tr}\big(\boldsymbol{\Sigma}_{\mathrm{r}}^{-1}(d\mathbf{A}_1)\mathbf{Y}_{t-1}\mathbf{B}_1^\top\boldsymbol{\Sigma}_{\mathrm{c}}^{-1}\mathbf{E}_t^\top\big) = \operatorname{tr}\big(\mathbf{Y}_{t-1}\mathbf{B}_1^\top\boldsymbol{\Sigma}_{\mathrm{c}}^{-1}\mathbf{E}_t^\top\boldsymbol{\Sigma}_{\mathrm{r}}^{-1}\,d\mathbf{A}_1\big)\,,$$

where the second step uses the cyclic property of the trace. Identifying $\boldsymbol{\Xi}_{\mathbf{A}_1} = \mathbf{Y}_{t-1}\mathbf{B}_1^\top\boldsymbol{\Sigma}_{\mathrm{c}}^{-1}\mathbf{E}_t^\top\boldsymbol{\Sigma}_{\mathrm{r}}^{-1}$ yields

$$\frac{\partial\ell_t}{\partial\mathbf{A}_1} = \boldsymbol{\Xi}_{\mathbf{A}_1}^\top = \boldsymbol{\Sigma}_{\mathrm{r}}^{-1}\mathbf{E}_t\boldsymbol{\Sigma}_{\mathrm{c}}^{-1}\mathbf{B}_1\mathbf{Y}_{t-1}^\top,$$

and therefore

$$\frac{\partial\ell_t}{\partial\operatorname{vec}(\mathbf{A}_1)} = \operatorname{vec}\big(\boldsymbol{\Sigma}_{\mathrm{r}}^{-1}\mathbf{E}_t\boldsymbol{\Sigma}_{\mathrm{c}}^{-1}\mathbf{B}_1\mathbf{Y}_{t-1}^\top\big) = \big[(\mathbf{Y}_{t-1}\mathbf{B}_1^\top\boldsymbol{\Sigma}_{\mathrm{c}}^{-1})\otimes\boldsymbol{\Sigma}_{\mathrm{r}}^{-1}\big]\operatorname{vec}(\mathbf{E}_t),$$

where the last equality uses $\operatorname{vec}(\mathbf{PQR}) = (\mathbf{R}^\top\otimes\mathbf{P})\operatorname{vec}(\mathbf{Q})$.

A.2 Score with respect to vec($\mathbf{B}_1$)

Now $d\mathbf{E}_t = -\mathbf{A}_1\mathbf{Y}_{t-1}(d\mathbf{B}_1)^\top$, hence $d\mathbf{E}_t^\top = -(d\mathbf{B}_1)\mathbf{Y}_{t-1}^\top\mathbf{A}_1^\top$. Arguing as above:

$$d\ell_t = \operatorname{tr}\big(\boldsymbol{\Sigma}_{\mathrm{r}}^{-1}\mathbf{E}_t\boldsymbol{\Sigma}_{\mathrm{c}}^{-1}(d\mathbf{B}_1)\mathbf{Y}_{t-1}^\top\mathbf{A}_1^\top\big) = \operatorname{tr}\big(\mathbf{Y}_{t-1}^\top\mathbf{A}_1^\top\boldsymbol{\Sigma}_{\mathrm{r}}^{-1}\mathbf{E}_t\boldsymbol{\Sigma}_{\mathrm{c}}^{-1}\,d\mathbf{B}_1\big)\,.$$

Identifying $\boldsymbol{\Xi}_{\mathbf{B}_1} = \mathbf{Y}_{t-1}^\top\mathbf{A}_1^\top\boldsymbol{\Sigma}_{\mathrm{r}}^{-1}\mathbf{E}_t\boldsymbol{\Sigma}_{\mathrm{c}}^{-1}$ yields

$$\frac{\partial\ell_t}{\partial\mathbf{B}_1} = \boldsymbol{\Xi}_{\mathbf{B}_1}^\top = \boldsymbol{\Sigma}_{\mathrm{c}}^{-1}\mathbf{E}_t^\top\boldsymbol{\Sigma}_{\mathrm{r}}^{-1}\mathbf{A}_1\mathbf{Y}_{t-1},$$

and therefore

$$\frac{\partial\ell_t}{\partial\operatorname{vec}(\mathbf{B}_1)} = \operatorname{vec}\big(\boldsymbol{\Sigma}_{\mathrm{c}}^{-1}\mathbf{E}_t^\top\boldsymbol{\Sigma}_{\mathrm{r}}^{-1}\mathbf{A}_1\mathbf{Y}_{t-1}\big) = \big[(\mathbf{Y}_{t-1}^\top\mathbf{A}_1^\top\boldsymbol{\Sigma}_{\mathrm{r}}^{-1})\otimes\boldsymbol{\Sigma}_{\mathrm{c}}^{-1}\big]\operatorname{vec}(\mathbf{E}_t^\top).$$

A.3 Score with respect to vech($\boldsymbol{\Sigma}_c$)

The matrices $\mathbf{A}_1$, $\mathbf{B}_1$, and $\boldsymbol{\Sigma}_{\mathrm{r}}$ are held fixed. Using $d(\boldsymbol{\Sigma}_{\mathrm{c}}^{-1}) = -\boldsymbol{\Sigma}_{\mathrm{c}}^{-1}(d\boldsymbol{\Sigma}_{\mathrm{c}})\boldsymbol{\Sigma}_{\mathrm{c}}^{-1}$:

$$\begin{aligned} d\ell_t &= -\frac{m}{2}\operatorname{tr}\big(\boldsymbol{\Sigma}_{\mathrm{c}}^{-1}\,d\boldsymbol{\Sigma}_{\mathrm{c}}\big) + \frac{1}{2}\operatorname{tr}\big(\boldsymbol{\Sigma}_{\mathrm{r}}^{-1}\mathbf{E}_t\boldsymbol{\Sigma}_{\mathrm{c}}^{-1}(d\boldsymbol{\Sigma}_{\mathrm{c}})\boldsymbol{\Sigma}_{\mathrm{c}}^{-1}\mathbf{E}_t^\top\big) \\ &= \operatorname{tr}\left(\underbrace{\left[-\frac{m}{2}\boldsymbol{\Sigma}_{\mathrm{c}}^{-1} + \frac{1}{2}\boldsymbol{\Sigma}_{\mathrm{c}}^{-1}\mathbf{E}_t^\top\boldsymbol{\Sigma}_{\mathrm{r}}^{-1}\mathbf{E}_t\boldsymbol{\Sigma}_{\mathrm{c}}^{-1}\right]}_{\mathbf{G}_c}\,d\boldsymbol{\Sigma}_{\mathrm{c}}\right), \end{aligned}$$

where we used the cyclic property to bring $\boldsymbol{\Sigma}_{\mathrm{r}}^{-1}\mathbf{E}_t$ to the right. The matrix $\mathbf{G}_c$ is symmetric, so restricting to the symmetric subspace via the duplication matrix gives

$$\frac{\partial\ell_t}{\partial\operatorname{vech}(\boldsymbol{\Sigma}_{\mathrm{c}})} = \mathbf{D}_n^\top\operatorname{vec}(\mathbf{G}_c) = -\frac{m}{2}\mathbf{D}_n^\top\operatorname{vec}(\boldsymbol{\Sigma}_{\mathrm{c}}^{-1}) + \frac{1}{2}\mathbf{D}_n^\top(\boldsymbol{\Sigma}_{\mathrm{c}}^{-1}\otimes\boldsymbol{\Sigma}_{\mathrm{c}}^{-1})\operatorname{vec}(\mathbf{E}_t^\top\boldsymbol{\Sigma}_{\mathrm{r}}^{-1}\mathbf{E}_t),$$

where the last equality uses $\operatorname{vec}(\boldsymbol{\Sigma}_{\mathrm{c}}^{-1}\mathbf{Q}\boldsymbol{\Sigma}_{\mathrm{c}}^{-1}) = (\boldsymbol{\Sigma}_{\mathrm{c}}^{-1}\otimes\boldsymbol{\Sigma}_{\mathrm{c}}^{-1})\operatorname{vec}(\mathbf{X})$ with $\mathbf{X} = \mathbf{E}_t^\top\boldsymbol{\Sigma}_{\mathrm{r}}^{-1}\mathbf{E}_t$.

A.4 Score with respect to vech($\boldsymbol{\Sigma}_r$)

An entirely symmetric argument, with the roles of $\boldsymbol{\Sigma}_{\mathrm{r}}$ and $\boldsymbol{\Sigma}_{\mathrm{c}}$ exchanged and n replaced by m, gives

$$\mathbf{G}_r = -\frac{n}{2}\boldsymbol{\Sigma}_{\mathrm{r}}^{-1} + \frac{1}{2}\boldsymbol{\Sigma}_{\mathrm{r}}^{-1}\mathbf{E}_t\boldsymbol{\Sigma}_{\mathrm{c}}^{-1}\mathbf{E}_t^\top\boldsymbol{\Sigma}_{\mathrm{r}}^{-1},$$

and therefore

$$\frac{\partial \ell_t}{\partial \operatorname{vech}(\boldsymbol{\Sigma}_{\mathrm{r}})} = \mathbf{D}_m^\top \operatorname{vec}(\mathbf{G}_r) = -\frac{n}{2}\mathbf{D}_m^\top \operatorname{vec}(\boldsymbol{\Sigma}_{\mathrm{r}}^{-1}) + \frac{1}{2}\mathbf{D}_m^\top(\boldsymbol{\Sigma}_{\mathrm{r}}^{-1} \otimes \boldsymbol{\Sigma}_{\mathrm{r}}^{-1}) \operatorname{vec}(\mathbf{E}_t \boldsymbol{\Sigma}_{\mathrm{c}}^{-1} \mathbf{E}_t^\top).$$

Stacking the four blocks and summing over $t = 2, \ldots, T$ recovers equation (14) in the main text.

B Proof of Proposition 1

Proof. The proof proceeds by applying the chain rule through four steps:

$\hat{\boldsymbol{\Sigma}}_{\mathrm{c}} \to \hat{\boldsymbol{\Sigma}}_{\mathrm{c}}^{-1} \to \hat{\mathbf{C}}_0^\top \to \hat{\mathbf{Q}}^{-\top} \to \operatorname{vecl}(\hat{\mathbf{Q}}^{-\top})$.

The first step concerns the Jacobian of matrix inversion, $\frac{\partial \operatorname{vech}(\hat{\boldsymbol{\Sigma}}_{\mathrm{c}}^{-1})}{\partial \operatorname{vech}(\hat{\boldsymbol{\Sigma}}_{\mathrm{c}})^\top}$. From the differential $d(\hat{\boldsymbol{\Sigma}}_{\mathrm{c}}^{-1}) = -\hat{\boldsymbol{\Sigma}}_{\mathrm{c}}^{-1}(d\hat{\boldsymbol{\Sigma}}_{\mathrm{c}})\hat{\boldsymbol{\Sigma}}_{\mathrm{c}}^{-1}$, vectorizing and reducing to vech via the duplication matrix $\mathbf{D}_n$ and its Moore–Penrose inverse $\mathbf{D}_n^+$:

$$\mathbf{J}_1 = \frac{\partial \operatorname{vech}(\hat{\boldsymbol{\Sigma}}_{\mathrm{c}}^{-1})}{\partial \operatorname{vech}(\hat{\boldsymbol{\Sigma}}_{\mathrm{c}})^\top} = -\mathbf{D}_n^+ (\hat{\boldsymbol{\Sigma}}_{\mathrm{c}}^{-1} \otimes \hat{\boldsymbol{\Sigma}}_{\mathrm{c}}^{-1}) \mathbf{D}_n.$$

Then, we compute the Jacobian of the Cholesky factor, $\frac{\partial \operatorname{vec}(\hat{\mathbf{C}}_0^\top)}{\partial \operatorname{vech}(\hat{\boldsymbol{\Sigma}}_{\mathrm{c}}^{-1})^\top}$. From the Cholesky decomposition of the precision matrix $\hat{\boldsymbol{\Sigma}}_{\mathrm{c}}^{-1} = \hat{\mathbf{C}}_0^\top \hat{\mathbf{C}}_0$, an infinitesimal perturbation gives

$$d\hat{\boldsymbol{\Sigma}}_{\mathrm{c}}^{-1} = d\hat{\mathbf{C}}_0^\top \hat{\mathbf{C}}_0 + \hat{\mathbf{C}}_0^\top d\hat{\mathbf{C}}_0.$$

Vectorizing both sides and using $\operatorname{vec}(\mathbf{ABC}) = (\mathbf{C}^\top \otimes \mathbf{A}) \operatorname{vec}(\mathbf{B})$ and $\operatorname{vec}(\mathbf{A}^\top) = \mathbf{K}_{nn} \operatorname{vec}(\mathbf{A})$ yields

$$\operatorname{vec}(d\,\hat{\boldsymbol{\Sigma}}_{\mathrm{c}}^{-1}) = \Big[(\hat{\mathbf{C}}_0^\top \otimes \mathbf{I}_n) + (\mathbf{I}_n \otimes \hat{\mathbf{C}}_0^\top)\mathbf{K}_{nn}\Big] \operatorname{vec}(d\hat{\mathbf{C}}_0^\top).$$

Since $\hat{\mathbf{C}}_0^\top$ is lower triangular, we use the elimination matrix to write $\operatorname{vec}(d\hat{\mathbf{C}}_0^\top) = \mathbf{T}_n \operatorname{vech}(d\hat{\mathbf{C}}_0^\top)$. Applying $\mathbf{D}_n^+$ to reduce the symmetric $\operatorname{vec}(d\,\hat{\boldsymbol{\Sigma}}_{\mathrm{c}}^{-1})$ to $\operatorname{vech}(d\,\hat{\boldsymbol{\Sigma}}_{\mathrm{c}}^{-1})$, we obtain

$$\operatorname{vech}(d\,\hat{\boldsymbol{\Sigma}}_{\mathrm{c}}^{-1}) = \hat{\mathbf{M}} \operatorname{vech}(d\hat{\mathbf{C}}_0^\top),$$

where $\hat{\mathbf{M}} = \mathbf{D}_n^+ \left[(\hat{\mathbf{C}}_0^\top \otimes \mathbf{I}_n) + (\mathbf{I}_n \otimes \hat{\mathbf{C}}_0^\top)\mathbf{K}_{nn}\right] \mathbf{T}_n$ is a square invertible matrix of dimension $\frac{n(n+1)}{2} \times \frac{n(n+1)}{2}$. Solving for $\text{vec}(d\hat{\mathbf{C}}_0^\top)$ and noting that $\text{vech}(d\,\hat{\mathbf{\Sigma}}_{\text{c}}^{-1}) = d\,\text{vech}(\hat{\mathbf{\Sigma}}_{\text{c}}^{-1})$, we get

$$\text{vec}(d\hat{\mathbf{C}}_0^\top) = \mathbf{T}_n\,\hat{\mathbf{M}}^{-1}\,d\,\text{vech}(\hat{\mathbf{\Sigma}}_{\text{c}}^{-1}),$$

which implies

$$\mathbf{J}_2 = \frac{\partial\ \text{vec}(\hat{\mathbf{C}}_0^\top)}{\partial\ \text{vech}(\hat{\mathbf{\Sigma}}_{\text{c}}^{-1})^\top} = \mathbf{T}_n\,\hat{\mathbf{M}}^{-1}.$$

The third step foresees the computation of the Jacobian of normalized inversion, $\frac{\partial\ \text{vec}(\hat{\mathbf{Q}}^{-\top})}{\partial\ \text{vec}(\hat{\mathbf{C}}_0^\top)^\top}$. From Equation (13), the unit lower triangular structural impact matrix is given by $\hat{\mathbf{Q}}^{-\top} = \hat{\mathbf{C}}_0^{-\top}\langle\hat{\mathbf{C}}_0\rangle$. Differentiating this mapping yields:

$$d\hat{\mathbf{Q}}^{-\top} = (d\hat{\mathbf{C}}_0^{-\top})\langle\hat{\mathbf{C}}_0\rangle + \hat{\mathbf{C}}_0^{-\top}(d\langle\hat{\mathbf{C}}_0\rangle).$$

Substituting $d\hat{\mathbf{C}}_0^{-\top} = -\hat{\mathbf{C}}_0^{-\top}(d\hat{\mathbf{C}}_0^\top)\hat{\mathbf{C}}_0^{-\top}$, we get

$$d\hat{\mathbf{Q}}^{-\top} = -\hat{\mathbf{C}}_0^{-\top}(d\hat{\mathbf{C}}_0^\top)\hat{\mathbf{C}}_0^{-\top}\langle\hat{\mathbf{C}}_0\rangle + \hat{\mathbf{C}}_0^{-\top}(d\langle\hat{\mathbf{C}}_0\rangle).$$

Since $\hat{\mathbf{Q}}^{-\top} = \hat{\mathbf{C}}_0^{-\top}\langle\hat{\mathbf{C}}_0\rangle$, we have

$$d\hat{\mathbf{Q}}^{-\top} = -\hat{\mathbf{C}}_0^{-\top}(d\hat{\mathbf{C}}_0^\top)\hat{\mathbf{Q}}^{-\top} + \hat{\mathbf{C}}_0^{-\top}(d\langle\hat{\mathbf{C}}_0\rangle).$$

Vectorizing and using $\text{vec}(\mathbf{ABC}) = (\mathbf{C}^\top \otimes \mathbf{A})\,\text{vec}(\mathbf{B})$ yields

$$\text{vec}(d\hat{\mathbf{Q}}^{-\top}) = -\left(\hat{\mathbf{Q}}^{-1} \otimes \hat{\mathbf{C}}_0^{-\top}\right)\text{vec}(d\hat{\mathbf{C}}_0^\top) + \left(\mathbf{I}_n \otimes \hat{\mathbf{C}}_0^{-\top}\right)\text{vec}(d\langle\hat{\mathbf{C}}_0\rangle).$$

Since $\langle\hat{\mathbf{C}}_0\rangle$ is a diagonal matrix, we can select its diagonal elements from $\hat{\mathbf{C}}_0^\top$ using selection matrices $\mathbf{H}_k = \boldsymbol{\eta}_k\boldsymbol{\eta}_k^\top$, where $\boldsymbol{\eta}_k$ is the k-th canonical basis vector of $\mathbb{R}^n$. Specifically, $\text{vec}(d\langle\hat{\mathbf{C}}_0\rangle) = \sum_{k=1}^n(\mathbf{H}_k \otimes \mathbf{H}_k)\,\text{vec}(d\hat{\mathbf{C}}_0^\top)$. Substituting this into the second term yields

$$\left(\mathbf{I}_n \otimes \hat{\mathbf{C}}_0^{-\top}\right)\sum_{k=1}^n(\mathbf{H}_k \otimes \mathbf{H}_k)\,\text{vec}(d\hat{\mathbf{C}}_0^\top) =$$
$$\sum_{k=1}^n\left(\mathbf{H}_k \otimes \hat{\mathbf{C}}_0^{-\top}\mathbf{H}_k\right)\text{vec}(d\hat{\mathbf{C}}_0^\top).$$

Therefore, combining both terms and factoring out $\mathrm{vec}(d\hat{\mathbf{C}}_0^\top)$ we obtain:

$$\mathbf{J}_3 = \sum_{k=1}^{n} \left(\mathbf{H}_k \otimes \hat{\mathbf{C}}_0^{-\top} \mathbf{H}_k \right) - \left(\hat{\mathbf{Q}}^{-1} \otimes \hat{\mathbf{C}}_0^{-\top} \right).$$

Combining via the chain rule:

$$\begin{aligned}
\mathbf{J} &= \mathbf{L}_n^s \cdot \mathbf{J}_3 \cdot \mathbf{J}_2 \cdot \mathbf{J}_1 \\
&= \mathbf{L}_n^s \left[\sum_{k=1}^{n} \left(\mathbf{H}_k \otimes \hat{\mathbf{C}}_0^{-\top} \mathbf{H}_k \right) - \left(\hat{\mathbf{Q}}^{-1} \otimes \hat{\mathbf{C}}_0^{-\top} \right) \right] \left(\mathbf{T}_n \hat{\mathbf{M}}^{-1} \right) \left(-\mathbf{D}_n^+ \left(\hat{\mathbf{\Sigma}}_{\mathrm{c}}^{-1} \otimes \hat{\mathbf{\Sigma}}_{\mathrm{c}}^{-1} \right) \mathbf{D}_n \right) \\
&= \mathbf{L}_n^s \left[\left(\hat{\mathbf{Q}}^{-1} \otimes \hat{\mathbf{C}}_0^{-\top} \right) - \sum_{k=1}^{n} \left(\mathbf{H}_k \otimes \hat{\mathbf{C}}_0^{-\top} \mathbf{H}_k \right) \right] \mathbf{T}_n \hat{\mathbf{M}}^{-1} \mathbf{D}_n^+ \left(\hat{\mathbf{\Sigma}}_{\mathrm{c}}^{-1} \otimes \hat{\mathbf{\Sigma}}_{\mathrm{c}}^{-1} \right) \mathbf{D}_n,
\end{aligned}$$

which exactly matches the result stated in Proposition 1. □